NASA CR-140303
ERIM 195100-1-F

Final Report

SIMULTANEOUS DUAL-BAND RADAR DEVELOPMENT

July 1972 Through April 1973

CHARLES L. LISKOW, et al.
Radar and Optics Division

SEPTEMBER 1974

Prepared for

NATIONAL AERONAUTICS AND SPACE ADMINISTRATION

Johnson Space Center, Houston, Texas 77058
Earth Observations Division

Contract NAS 9-12967

ENVIRONMENTAL
RESEARCH INSTITUTE OF MICHIGAN
FORMERLY WILLOW RUN LABORATORIES, THE UNIVERSITY OF MICHIGAN
BOX 618 • ANN ARBOR • MICHIGAN 48107

NOTICES

Sponsorship. The work reported herein was conducted by the Environmental Research Institute of Michigan for the National Aeronautics and Space Administration, Johnson Space Center, Houston, Texas 77058, under Contract NAS 9-12967. Mr. B. R. Baker/TF3 was the NASA Technical Monitor. Contracts and grants to the Institute for the support of sponsored research are administered through the Office of Contracts Administration.

TECHNICAL REPORT STANDARD TITLE PAGE

1. Report No.	2. Government Accession No.	3. Recipient's Catalog No.

4. Title and Subtitle	5. Report Date
SIMULTANEOUS DUAL-BAND RADAR DEVELOPMENT	September 1974
	6. Performing Organization Code
7. Author(s)	8. Performing Organization Report No.
C. L. Liskow, et al.	195100-1-F
9. Performing Organization Name and Address	10. Work Unit No.
Environmental Research Institute of Michigan Radar and Optics Division P.O. Box 618 Ann Arbor, MI 48107	11. Contract or Grant No. NAS 9-12967
	13. Type of Report and Period Covered Final Report, July 1972 through April 1973
12. Sponsoring Agency Name and Address	14. Sponsoring Agency Code
National Aeronautics and Space Administration Johnson Space Center Earth Observations Division Houston, Texas 77058	

15. Supplementary Notes

Mr. B. R. Baker/TF3 was the NASA Technical Monitor.

16. Abstract

Efforts of the ERIM Radar and Optics Division to design and construct an airborne imaging radar operating simultaneously at L and X-bands for NASA, JSC, at Houston, Texas under Contract NAS 9-12967 are described. This system combines much of the L and X-band radar equipment previously constructed under contract NAS 9-11306 with an all-inertial navigation system in order to form a dual-band radar system. The areas of development include duplex transmitters, receivers, and recorders, a control module, motion compensation for both bands, and adaptation of a commercial inertial navigation system. Also, installation of the system in the aircraft and flight tests are described. Circuit diagrams, performance figures, and some radar images are presented.

17. Key Words	18. Distribution Statement
Coherent radar Side-looking radar Radar imagery	Initial distribution is listed at the end of this document.

19. Security Classif. (of this report)	20. Security Classif. (of this page)	21. No. of Pages	22. Price
UNCLASSIFIED	UNCLASSIFIED	60	

PREFACE

The work reported in this final report was sponsored by the Earth Observations Division of the NASA Johnson Space Center, Houston, Texas under Contract NAS 9-12967 and was performed by the Radar and Optics Division of the Environmental Research Institute of Michigan (ERIM), Ann Arbor, Michigan. This program was a follow-on to work done previously under Contract NAS 9-11306.

The NASA technical monitor for this program was Mr. B. R. Baker/ TF3, and the ERIM principal investigator was Mr. Robert A. Rendleman. The technical responsibilities of the various authors were as follows: control module (R. W. Bayma), transmitter and receiver (R. J. Salmer and F. L. Smith), recorders (C. D. Stout), data processing (J. M. Marks), navigation and motion compensation (M. B. Evans), installation and flight test (R. F. Rawson and F. L. Smith), imagery interpretation (C. L. Liskow), and report coordination (C. L. Liskow).

The contract covered the period from 1 July 1972 through 30 January 1973. The research work reported herein extended into April of 1973; the later effort was supported under separate sponsorship.

The ERIM number for this report is 195100-1-F.

CONTENTS

FIGURES

TABLES

SIMULTANEOUS DUAL-BAND RADAR DEVELOPMENT

1
INTRODUCTION

Under NASA sponsorship in 1971 (Contract NAS 9-11306), an X-band airborne radar was modified to operate at L-band as well [1]. Frequency converters, an L-band transmitter and receiver, and an L-band antenna were added to the X-band radar installation in the C-46 aircraft to allow the system to image terrain with either L or X-band radiation (but not both simultaneously). The modification was made to provide dual-band operation quickly and with limited expense. Radar imagery of an area with both radiation frequencies could be obtained only by flying past the target area twice. This is not only time-consuming and expensive, but also one could never be certain that the target area was unchanged between passes.

In 1972, a second contract was written (Contract NAS 9-12967) with a completion date of January 30, 1973. The goal of this second development program was the design and construction of an airborne radar system that would collect simultaneous dual-frequency and dual-polarization radar imagery data. The resulting four-channel output imagery thus displays the target swath four ways: X-band parallel-polarized, X-band cross-polarized, L-band parallel-polarized, and L-band cross-polarized. This follow-on program is the subject of this report.

The system design uses one dual-channel recorder for X-band signals and another dual-channel recorder for L-band signals. This arrangement precludes simultaneous recording of the two polarization components from a single transmitted pulse (since they must occur at different times in order to fit onto the two sides of the recorder sweep). One transmitter pulse is required for each of the four channels. Thus, the system employs a four-pulse sequence in which the transmitters are active on alternate pulses, and the four receiving and recording channels are switched on sequentially (i.e., each of the four receiver channels is active on every fourth pulse). The motion-compensation phase-shift scale factor is changed on each pulse in order to be compatible with the radiation wavelength. All of these functions that change during the four-pulse sequence are controlled by a newly-developed Control Module (CM). Four output images are produced by processing each recorded data channel separately on a high-quality optical processor.

The basic radar technique utilized by the new system remains essentially as it was in the 1971 system [1] and is as follows: An FM ("chirp") pulse of microwave radiation is emitted and echoes of both polarizations are received and synchronously detected. These signals are

displayed on CRT faces and recorded on continuously-moving photographic film as a series of adjacent intensity-modulated traces. The resulting data storage films have chirp modulation in the range (across-the-film) direction and Doppler modulation in the cross-range (along-the-film) direction. A ground-based optical processor is used to perform two-dimensional pulse compression and thus to produce an output image which is recorded on an output film.

The heterodyning scheme used in the previous X- or L-band radar is retained in the present simultaneous dual-band radar. This avoids the design and construction of additional critical, high-stability components.

Both antenna beams are oriented to the zero-Doppler line (perpendicular to the desired ground track) during data-collection flights. Electronic offset is added to the X-band signals in the cross-range dimension. The L-band signals have offset in the range dimension.

The Doppler-inertial system that had been used to stabilize the antenna, guide the aircraft, and sense lateral motion of the antenna was replaced with an all-inertial navigation system. The inertial system is both smaller and lighter than the previous system, but adapting this commercially-available equipment to the radar required some design and development effort.

Development of the various radar components required for the dual-band radar consumed more time than had been anticipated. As a result, installation of the complete dual-band radar system in the laboratory aircraft was completed after the contract termination date, and flight testing was not started until March 1973. Multi-channel imagery was obtained, but several operational problems were evident. Effort was applied to analyzing and repairing the deficiencies, and additional flights were made later in 1973. Significant improvement in imaging performance resulted.

2
CONTROL MODULE

The dual-band, dual-polarization radar combines a number of subsystems, as shown in Figure 1. (The L-band portions of the radar are set off by a dashed line, and the Control Module is set off by a solid line.) These subsystems form a working radar system which is directed by the Control Module (CM).

2.1 DESIGN CONCEPTS

Figure 2 shows the timing sequence of the various radar functions controlled by the CM in mode 4, which is its normal mode of operation. A complete four-pulse sequence is illustrated, with time increasing to the right. Radar trigger pulses are shown in the top four lines; the remaining lines describe signals which are generated and/or controlled by the CM.

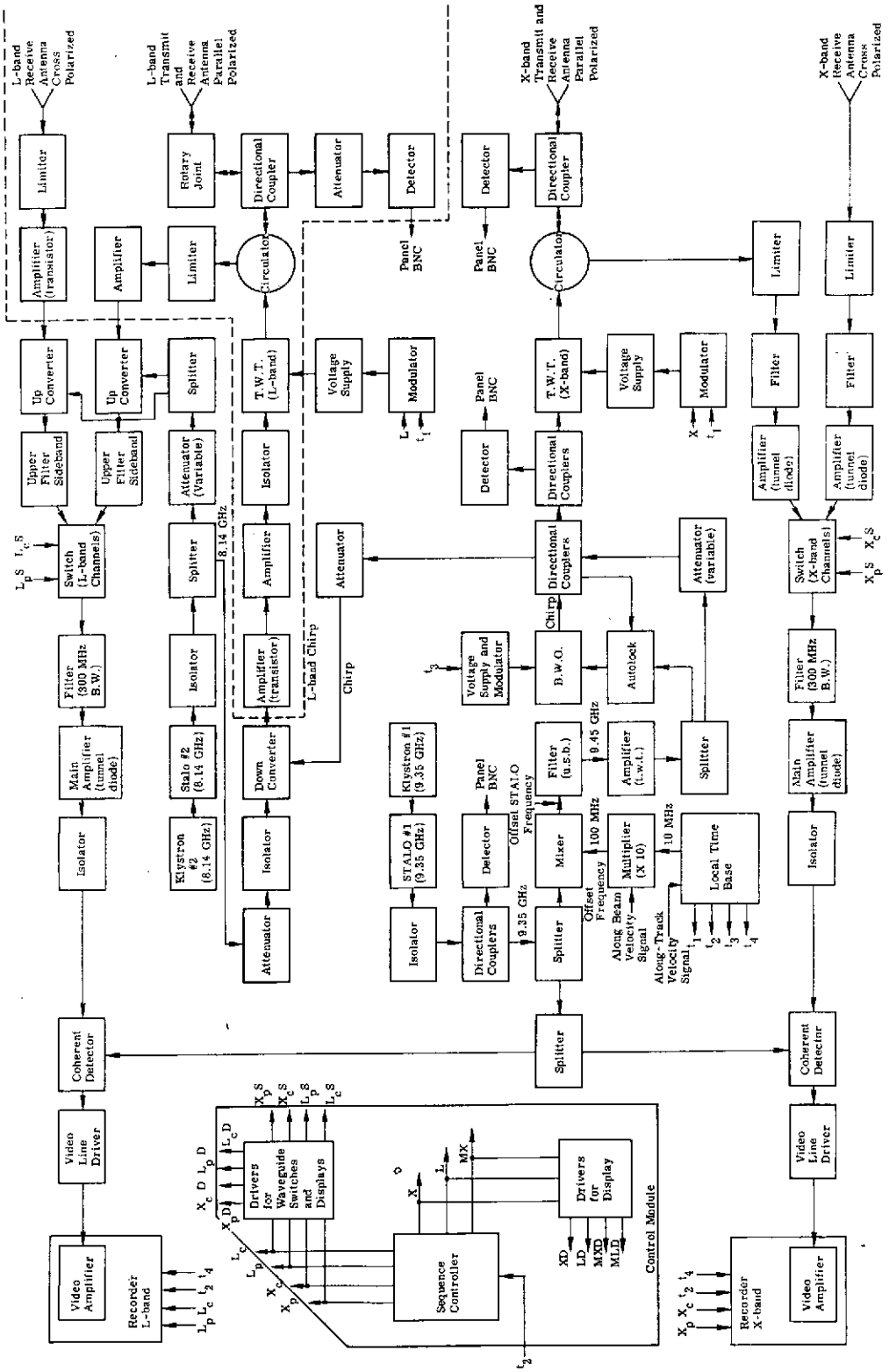

FIGURE 1. DUAL-BAND RADAR BLOCK DIAGRAM

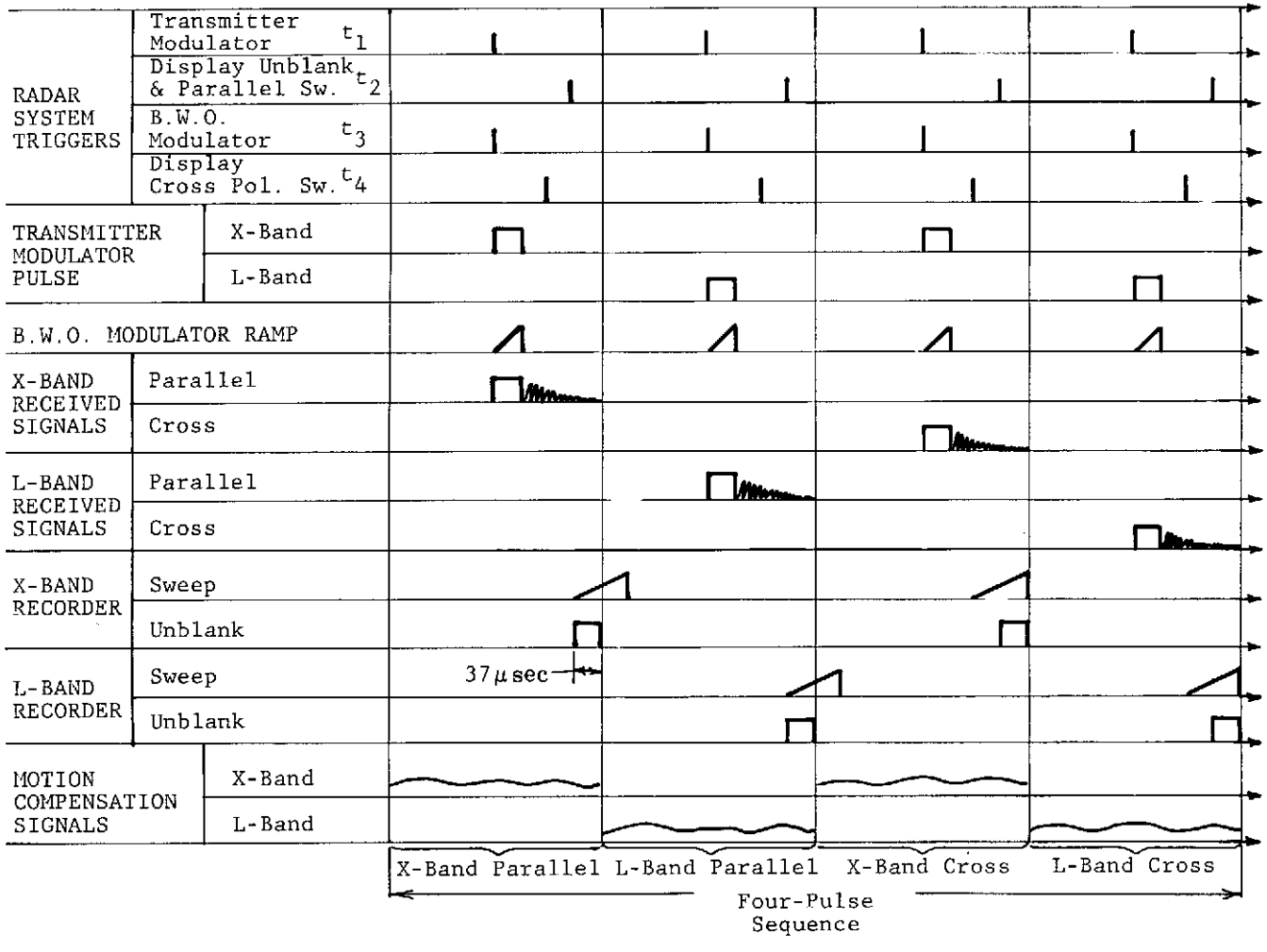

FIGURE 2. TIMING SEQUENCE OF DUAL-BAND RADAR

Direction provided by the CM includes control of the operating sequence of the transmitters, receivers, and recorders as well as the motion-compensation scale used in the radar. Radar functions which require accurate timing are triggered by supplying CM gating signals (having uncritical timing) to the appropriate subsystems to permit or deny the entrance of accurately-timed radar trigger pulses. In this way, none of the CM circuitry is required to maintain the high timing accurately of the radar system triggers, and no compromise of trigger accuracy is caused by routing the triggers through the CM. In some cases where accurate triggers are not required, the CM supplies the control signals directly.

The CM is triggered by a delayed radar system trigger pulse recurring at the system pulse repetition frequency (PRF), which is four times the single-channel PRF. The outputs of the CM are a set of signals which sequentially reconfigure the radar subsystem to operate in one of four configurations: X-band parallel-polarized (X_p), X-band cross-polarized (X_c), L-band parallel-polarized (L_p), or L-band cross-polarized (L_c).

The delayed system trigger t_2 that is used to synchronize the CM is delayed from the transmitter trigger t_1 by a time interval that determines the range to the near edge of the displayed terrain swath. This trigger is further delayed within the CM by a fixed 40 μsec in order to have all the control gates change just after the 37 μsec recording period.

The trigger pulse repetition rate is divided by four to generate a four-pulse operating sequence with four time slots: TS(0), . . . , TS(3), one for each of the required four configurations. A complete list of operating modes is shown in Table 1.

Control signals from the CM are routed to several widely separated radar-subsystem units in the aircraft. In order to prevent noise problems associated with cross-talk, ground loops, etc., all remote signal couplings were made by means of photo-optic isolators (light-coupled relays). As a result, no signal transfer problems have occurred.

A second design choice was to implement the control logic as inhibit signals; i.e., subsystem operation is inhibited during non-selected time slots by an active control signal. This simplifies subsystem upkeep by permitting normal checkout and maintenance without the need of the CM unit.

A third design consideration was adaptability. The selected sequencing mode is controlled by a readily replaceable read-only memory (ROM). Thus, the operating sequence (assignment of operating mode to time slot) can be changed by programing a replacement ROM without changing CM wiring.

An additional feature of the CM is the conditional fail-safe monitoring system incorporated into it. The generated control signals are continuously monitored by a light emitting diode (LED) display. An open or short circuit in the control lines will turn off the corresponding LED

TABLE 1. OPERATING SEQUENCES AND TIME-SLOT ASSIGNMENT

Mode	Designation	Time Slot TS(0)	TS(1)	TS(2)	TS(3)
M(0)	OFF	--	--	--	--
M(1)	$X_{\perp}$	--	--	XC	--
M(2)	$X_{\|\|}$	XP	--	--	--
M(3)	$X_{\|\|}X_{\perp}$	XP	--	XC	--
M(4)	$X_{\|\|}L_{\|\|}X_{\perp}L_{\perp}$	XP	LP	XC	LC
M(5)	$L_{\|\|}L_{\perp}$	--	LP	--	LC
M(6)	$L_{\|\|}$	--	LP	--	--
M(7)	$L_{\perp}$	--	--	--	LC

element, thus indicating a subsystem failure. In addition, logic is included which automatically inhibits radar subsystem operation in the event of trigger loss.

2.2 CIRCUIT DETAILS

A block diagram of the Control Module showing major logic and control signals is given in Figure 3. The input trigger t_2, which determines the start of the recorded signal period, is delayed by 40 μsec by a monostable multivibrator to trigger the sequence controller after each 37 μsec record interval. The trigger rate is divided by four in a two-stage binary counter with logic outputs C0 and C1. The position of the Mode Control Switch is coded as three binary bits, C2, C3 and C4. The combined five-bit word (C0, . . . , C4) addresses the ROM to select an eight-bit control word (B0, . . . , B7). Bits one through seven (B1, . . . , B7) are used to generate the control signals; bit zero (B0) is not used.

Logic signals X and L gate the respective transmitters. Logic signals X_p, X_c, L_p, and L_c gate the respective recorder channels and, through parallel channels, control signals X_pS, X_cS, L_pS, and L_cS operate the respective receiver waveguide switches. These control signals are 30 mA current sources (at approximately +4 V) when the respective waveguide switches are open (maximum insertion loss), and -18 V reverse-bias sources when the switches are closed (minimum insertion loss); this provides the active inhibit feature described in Section 2.1. Logic signal MX gates the motion-compensation scale control (when MX is high, X-band motion compensation is used; when MX is low, L-band motion compensation is used). Logic signals XD, LD, X_pD, X_cD, L_pD, L_cD, MXD and MLD (MLD = $\overline{\text{MXD}}$) drive the corresponding LED displays. The signals are low when the display is activated.

The entire CM circuit, including power-supply filters and regulators, is constructed on three 4 × 6 in. printed circuit cards. TTL logic is used throughout except for the waveguide switch drivers which are made of discrete components. After initial construction, an additional circuit card was added to provide selectable oscilloscope sync signals for transmitter, receiver, and recorder monitoring purposes. This circuit is peripheral to the CM operation and is therefore not shown in Fig. 3.

3
TRANSMITTER

The twin transmitters used in the dual-band radar use two traveling-wave tubes as final amplifiers, one at X-band and the other at L-band (see Fig. 1). These output stages amplify intermediate-level frequency-modulated pulses to one and five kW levels, respectively. The source of the FM pulses to drive these amplifiers is a stabilized X-band BWO which is frequency

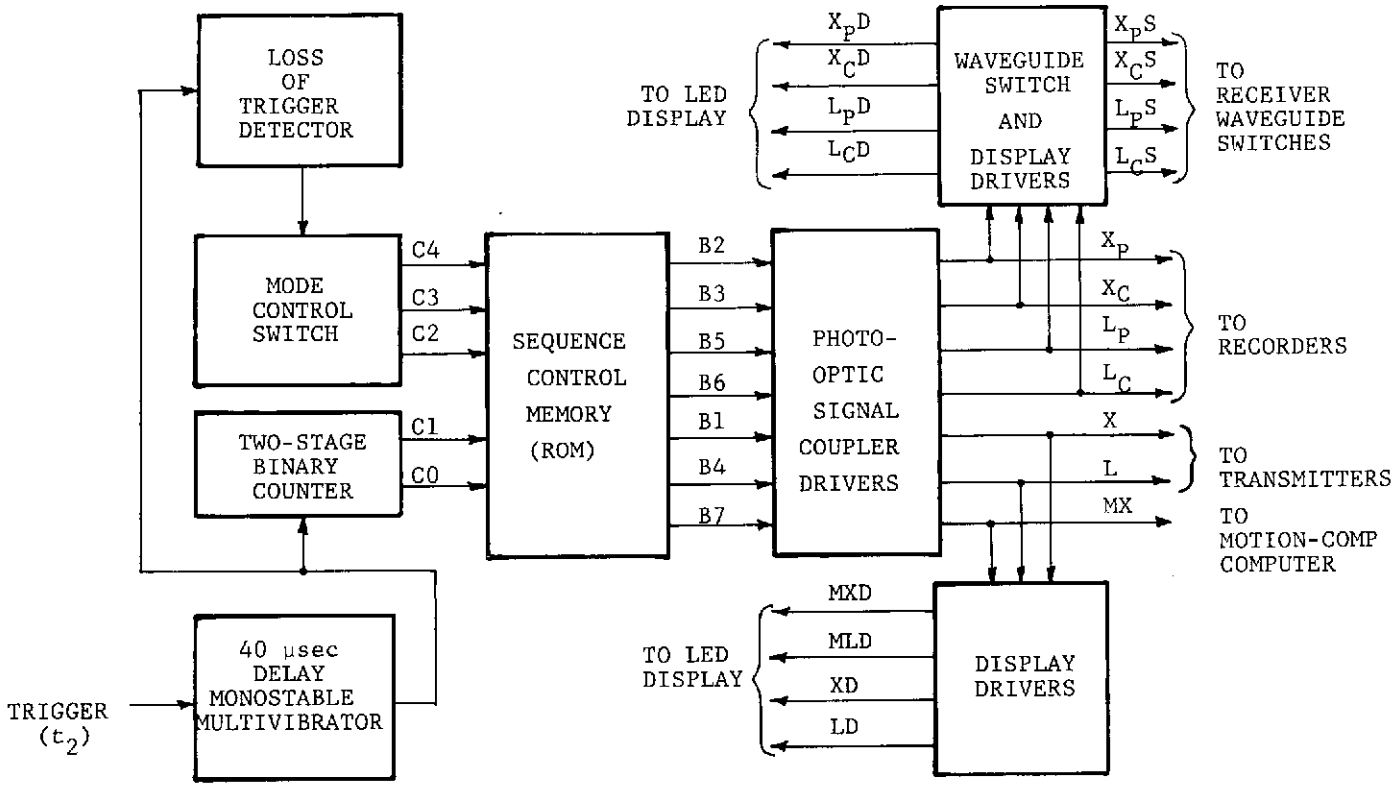

FIGURE 3. CONTROL MODULE BLOCK DIAGRAM

modulated by means of a ramp voltage pulse on its helix. The X-band pulse is (1) fed directly to the X-band TWT for X-band transmission, and (2) heterodyned to L-band and filtered (in the down converter), amplified, and fed to the L-band TWT for L-band transmission.

A major portion of the transmitter development effort was devoted to the design and implementation of the circuitry required for alternate-pulse operation of the X- and L-band transmitter tubes at the desired rate. This development effort centered on two subsystems common to both transmitters: (1) the modulators that pulse the output traveling-wave tubes, and (2) the various voltage supplies required by these tubes. These subsystems were used in the 1971 system by switching them to one or the other transmitter tube as needed. Accordingly, only one radar could be operated at one time.

Since the present system employs a four-pulse, four-mode sequence (described in Section 1), the duty factor of each transmitter was doubled as compared to the 1971 system. The existing modulator was marginal when it was used with each radar separately. Thus, with the increased duty factor of the new dual-frequency system, the modulator had to be redesigned.

3.1 MODULATOR REDESIGN

The primary goal to be realized in the redesign of the modulator was the increased duty-cycle capability. Improved reliability and ease of operation were important additional goals. Finally, it was necessary that the modulator generate a 300 V, 4μsec pulse for the X-band and L-band TWT grids which operate at -11 kV DC with respect to ground. The design objectives are shown in Table 2.

Figure 4 shows a schematic diagram of the modulator. The first integrated circuit (IC_1) is a light-coupled relay which turns the second integrated circuit (IC_2) on or off depending upon the level of the logic signal from the CM. IC_2 is a monostable multivibrator which forms a 37μsec pulse starting at the coincidence of the radar system trigger t_1 and the enabling gate from IC_1. This pulse is amplified in Q_1; the amplified pulse then drives the base of the switch Q_2 in series with the inductor. The inductive energy-storage technique used here has the advantage that the silicon power transistor Q_2 is operated in its unsaturated mode before and during the pulse. IC_3 and Q_3 form a variable-voltage, shunt-regulated power supply. The voltage across the inductor is clamped to this supply to control amplitude and to create a flat pulse. The energy stored in the inductor is switched into an output pulse transformer at a rate controlled by the clamping circuit. This transformer isolates the modulator chassis from the TWT grid and thus avoids the necessity of floating the modulator at a high negative voltage with respect to ground. Both modulators are powered by the same 6 V, 9 A supply.

All objectives were met with this design with the exception of the lower values of duty cycle. Duty cycles achieved ranged from 0.2% to 3%. No serious operational problem is presented by this limitation, however, because the radar never operates below 0.2%. This limitation, of

TABLE 2. MODULATOR DESIGN OBJECTIVES

Pulse voltage amplitude	0 to 300 V
Pulse current	0 to 500 mA
Duty cycle	0 to 2%
Rise time	0.1 μsec
Pulse length	1.5 to 4.0 μsec
Fall time	0.1 μsec
Flatness	1%
Droop	1%
Ringing and overshoot	2%
Settling time	0.2 μsec
Isolation from ground to output	-25 kV
Weight	20 lb max. (2 units)

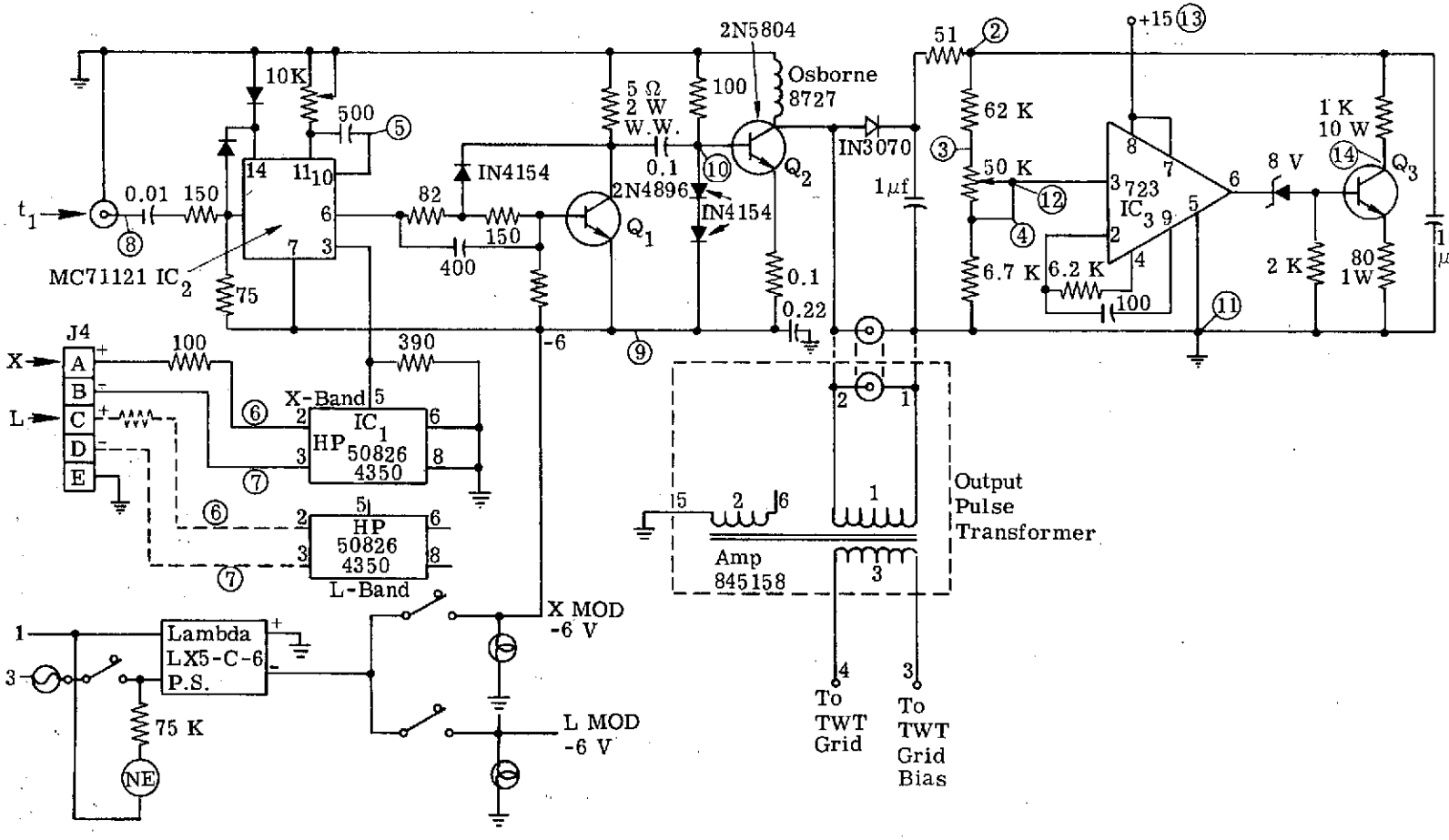

FIGURE 4. TRANSMITTER MODULATOR DIAGRAM

course, means that laboratory testing of the modulators must be done above 0.2% duty. In addition to meeting the performance goals, a major consequence of the redesign is reliability: both new modulators have given uninterrupted service.

3.2 TWT SUPPLIES

The TWT beam and "vac-ion" supplies were implemented by slight modifications to the existing units. The high-voltage beam supply provides the energy for the traveling wave interaction. The TWT anode is grounded and a negative high voltage is applied to the cathode; the X-band supply provides 50 mA at -11 kV, and the L-band supply provides 50 mA at -9.5 kV. The beam supply characteristics are:

Voltage	0-12.5 kV
Current	0-50 mA
Ripple	10 V max (p-p)

The high-voltage beam supply consists of a three-phase bridge rectifier, a choke-input filter (L_{in} = 40 H), and a one μf capacitor. The supply is not regulated. Heater, vac-ion, and cooling air interlocks are provided. The output voltage is controlled by an auto-transformer input to the high-voltage transformer.

"Vac-ion" pumps are used to hold the necessary hard vacuum in the TWTs. This pump is essentially a very-low-volume vacuum pump which removes ions from the TWT by means of electric and magnetic fields. The ion current in the pump is amplified in order to operate a relay in the high-voltage beam supply; when the original current exceeds 10 mA, the relay opens in order to remove the beam voltage from the TWT. The pump supplies are commercial units which provide 3 kV at 100 μA. The supply characteristics are:

Voltage	3 kV (±10%)
Current	0 to 100 μA
Output impedance	3 MΩ min

Because of the grounded anode mode of operation, two floating supplies with 12.5 kV isolation are required: (1) for the grid bias of -100 to -240 V with respect to the cathode, and (2) for the heaters which operate at 6 and 12 V. The design characteristics are shown in Table 3. The different grid biases required by the two different TWTs dictated a variable supply in place of the fixed voltage supply previously employed.

Figure 5 shows the circuit diagram for the X-band bias and heater supply. This circuit floats at a high negative voltage and is isolated from ground by means of the input power transformer (left) and the modulator output pulse transformer (right). This supply was modified by adding a regulated DC heater supply, which eliminates the need for the magnetic regulator previously employed in the primary of the input power transformer. (This modification could

TABLE 3. TWT SUPPLIES DESIGN CHARACTERISTICS

Grid Bias Supplies	
Voltage	-100 to -240 V
Current	0 - 2 mA
Sink	0 - 20 mA
Ripple	0.5 V max (p-p)
Isolation	-12.5 kV
Heater Supply (X-band)	
Voltage	6.3 V (± 2% rms)
Current	2.0 A (± 20%)
Isolation	-12.5 kV
Heater Supply (L-band)	
Voltage	12.0 V (± 2% rms)
Current	4.0 A (± 20%)
Isolation	-12.5 kV

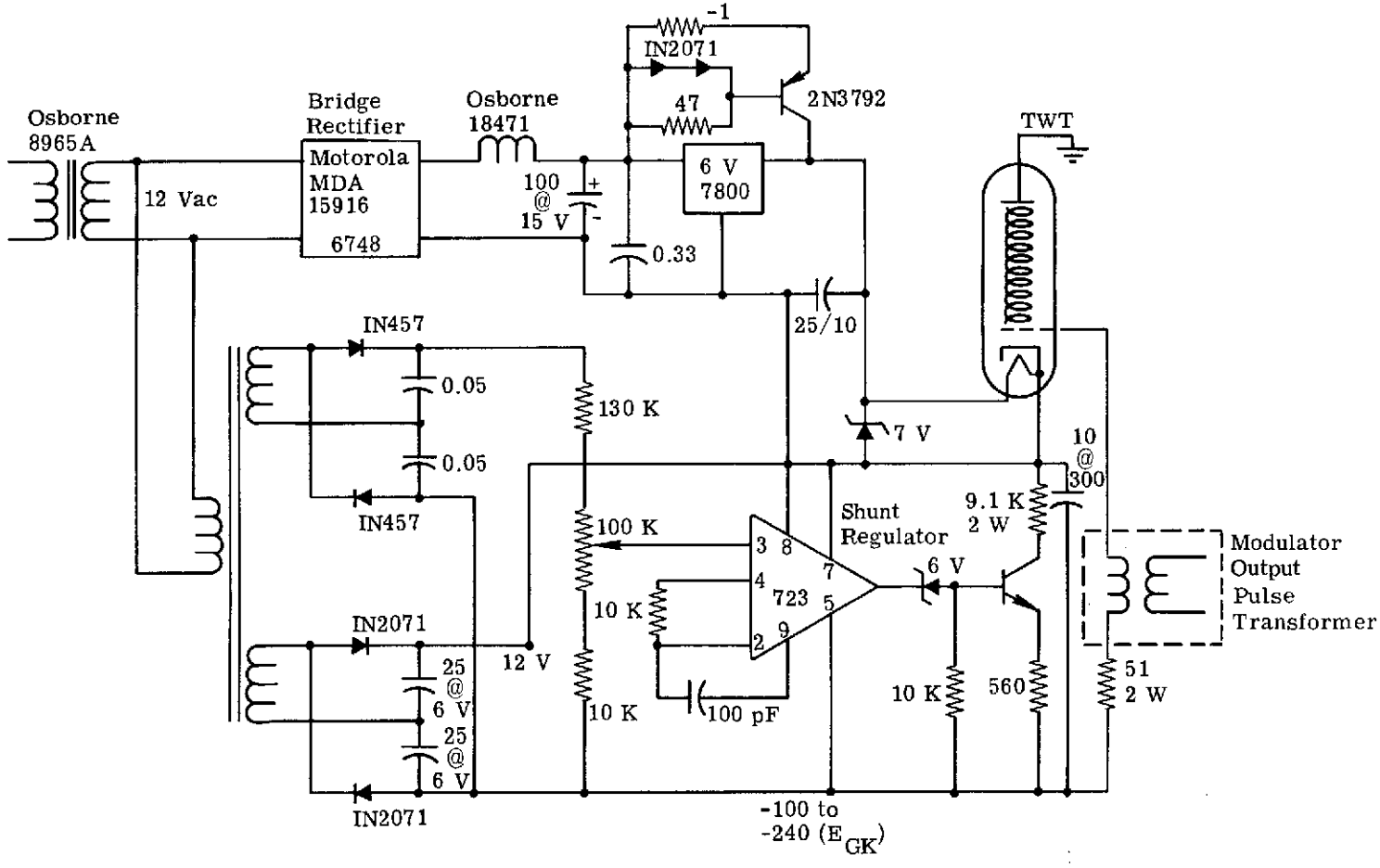

FIGURE 5. BIAS AND HEATER SUPPLY DIAGRAM (X-BAND)

not be made in the L-band supply because the L-band TWT heater requires 12 V, leaving insufficient voltage available for a DC regulator. This heater is therefore operated directly from the input transformer's 12 V AC secondary winding.) The X-band heater supply includes a bridge rectifier, a choke-input filter, and an integrated circuit regulator.

A separate grid bias is provided (rather than self-biasing) in order to avoid unstable operation of the TWT's during tube warm-up. The input to this supply is obtained from the 12 V input secondary winding, from which point it is stepped up to about 150 V (in a second transformer), rectified, and doubled. This voltage is then shunt regulated and applied to the grid of the TWT. Any grid current is dissipated through the shunt regulator. The shunt regulator is similar to the clamp supply used in the modulators. This grid bias supply circuit is used for both X and L-band.

3.3 STALO AND CHIRP

Considerable effort was devoted to developing a solid-state STALO and chirp-pulse generator, but it was finally decided that the existing vacuum-tube designs would be retained. The swept-frequency generator used in the radar transmitter to generate the chirp pulse was updated by installing a new voltage supply, a new phase-lock circuit, and an automatic-frequency-control (AFC) circuit. The BWO Auto-Lock system includes the phase-lock and AFC circuits; a block diagram is shown in Figure 6. This section is conceptually the same as in the earlier model, but it is different in instrumentation detail.

The objective of this control circuitry is to lock the BWO to the STALO during the period prior to the onset of each chirp signal so that the swept-frequency signal will start out at the correct frequency and phase. The phase-lock circuit is straight forward, and uses only a phase comparator (mixer) to determine the relative phase between the BWO and the STALO signals. Both sign and magnitude of phase difference are indicated by the output of this mixer, and the error signal is amplified and applied as a control signal to the BWO to maintain phase lock.

When the BWO frequency is different from the STALO frequency, a bipolar video signal exists at the output of the phase-lock mixer. The distance from lock is proportional to the frequency, but no direction information exists; thus, as the frequency difference increases, the video signal runs rapidly out of the passband of any reasonable video amplifier. The BWO frequency would stay only within a few hundred MHz of the STALO without control circuitry, and a phase-lock loop alone will neither hold nor capture control of the BWO. Therefore, an FM discriminator is used with a feedback loop to hold the BWO frequency within phase-lock range. The phase-lock and frequency-control functions had been combined in a single waveguide circuit in previous designs. This combined arrangement prevented either function from being optimized and made the adjustment process very difficult. The two functions were separated in the new design and improved performance has resulted.

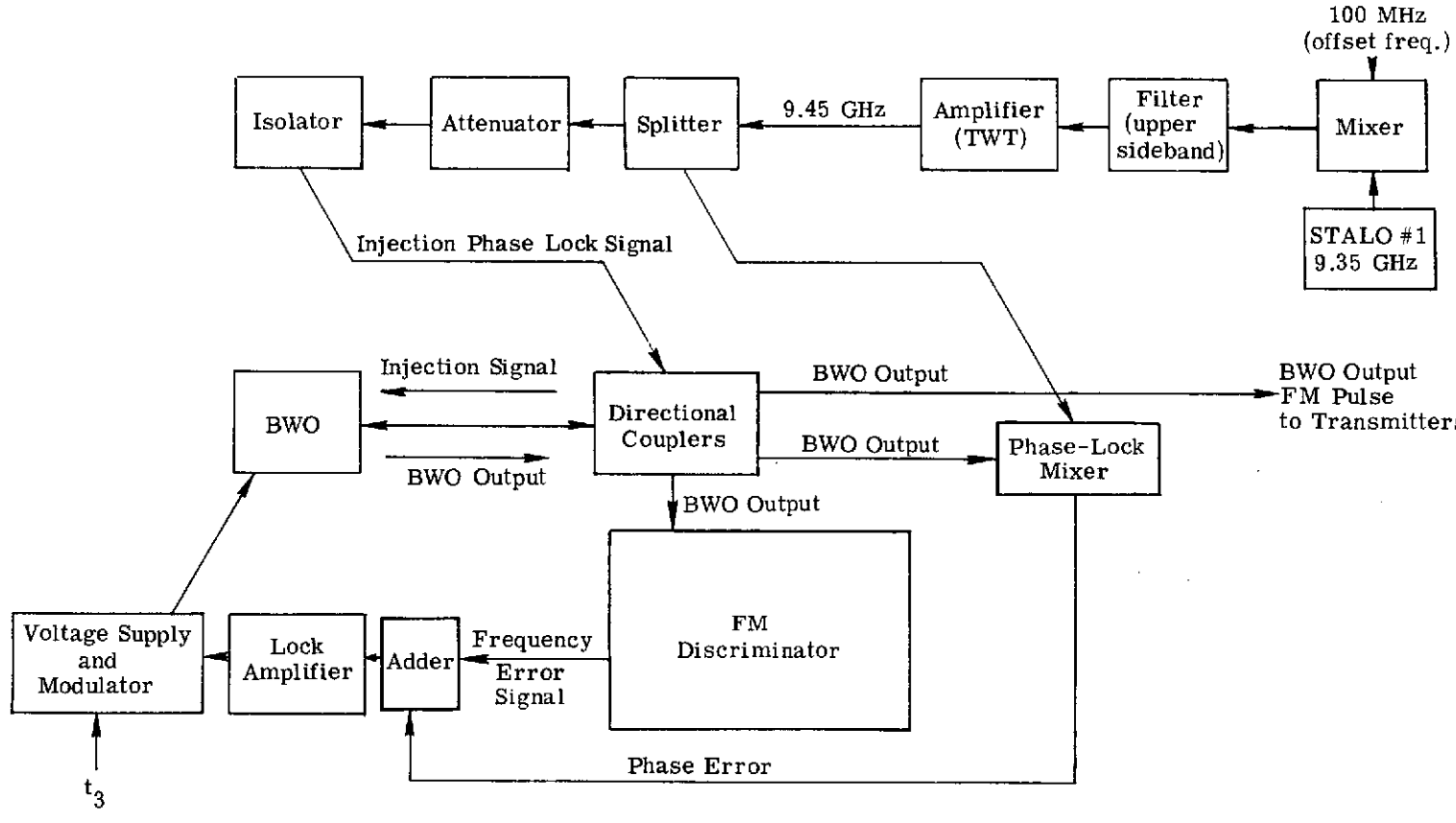

FIGURE 6. BLOCK DIAGRAM OF BWO AUTO-LOCK

The STALO is the reference X-band frequency for the radar system (both bands) and is shown at the upper right in Figure 6. Since the X-band portion of the radar uses a folded-spectrum technique, the BWO is stabilized to a frequency 100 MHz away from the STALO frequency. This offset is accomplished by beams of a 100 MHz offset frequency, a mixer, and a filter. This offset X-band signal is fed to the FM discriminator and to the phase-lock mixer; it is also fed to the BWO in order to add the beneficial effect of injection locking.

Figure 7 shows the wide-band capture range of the frequency-control circuit, and Figure 8 shows the combined frequency-control and phase-lock signals as the BWO is scanned through the auto-lock region.

4
RECEIVER

In the development of the receivers for the dual-band radar, emphasis was placed on those modifications necessary to implement the recorder polarization-duplexing function. In addition, other improvements were made in the receivers themselves, including improved noise figure and channel gain matching.

Two receiver channels had been employed previously to carry different polarization components simultaneously. Each channel operated in conjunction with its own recorder without duplexing. In the simultaneous dual-band system, four separate channels had to be provided and duplexed onto two recorders.

As shown in Figure 1, the dual-band receiver inputs consists of four separate channels extending to the left from the antenna arrays at the right. The two L-band channels are heterodyned (in the up converters) to X-band after initial amplification. One tunnel-diode amplifier stage was added in front of each leg of the waveguide switch in the X-band receiver to improve the noise figure. The four channels are then connected to two double-throw X-band waveguide switches which are programed to connect them sequentially into two X-band main amplifiers. (The desired channel is selected for each radar pulse period by the switch drive signals which come from the control module. The timing sequence is shown in Fig. 2.) These two amplifiers each connect to a coherent detector where the radar information is converted to video. The video signals are amplified and fed to the L-band and X-band recorders for data storage on photographic film.

Each receiver channel in the 1971 system used a traveling-wave tube for its main amplifier. The noise figure of one of these tubes had seriously degraded with age and use, and the gains of both were low. Accordingly, the dual-band receivers were redesigned with tunnel-diode amplifiers. The four channels were then optimized for gain match and limiting characteristics.

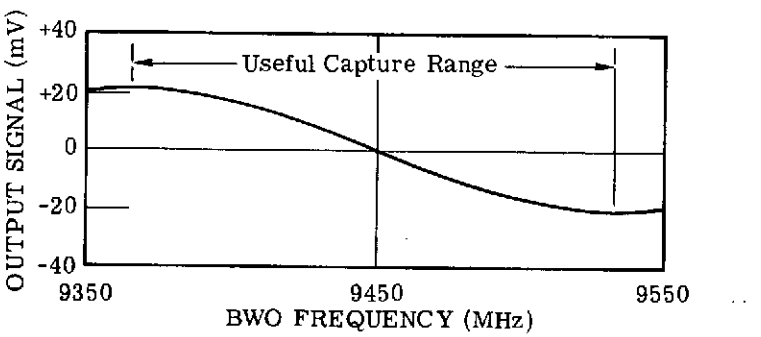

FIGURE 7. FM DISCRIMINATOR TRANSFER CHARACTERISTIC

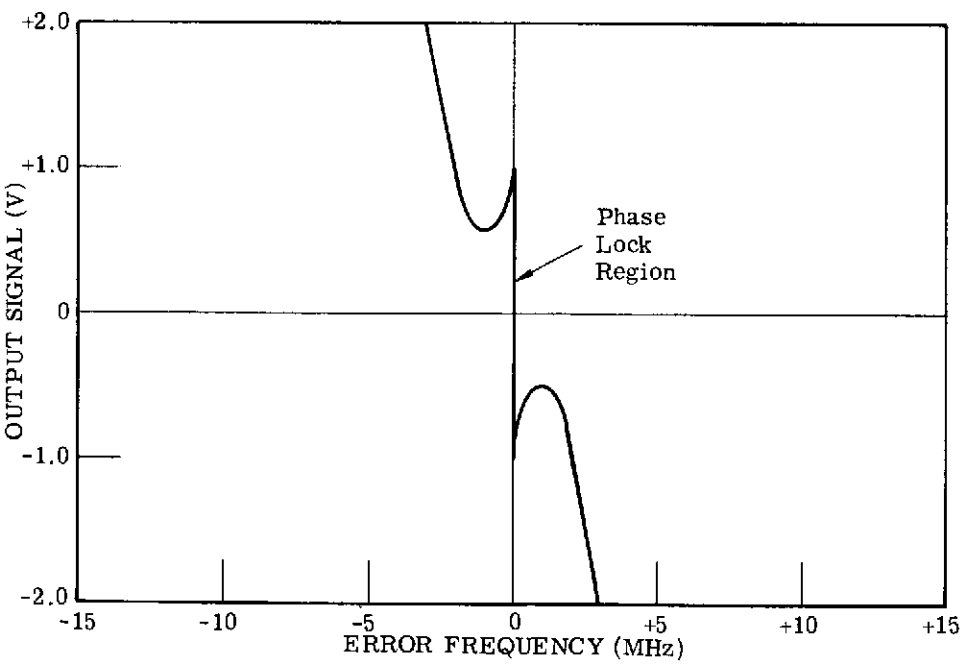

FIGURE 8. BWO LOCK AMPLIFIER OUTPUT VS. ERROR FREQUENCY

Measured transfer characteristic curves for the receivers are shown in Figures 9, 10, 11, and 12. Note that (1) the saturation levels are nearly equal, (2) there are some minor gain differences, and (3) there are some noise-level differences.

5
RECORDERS

The two duplexed recorders used in the dual-band, four-channel radar were adapted from the two single-channel recorders already in the radar aircraft. The physical layout of the recorders (including the CRT, the two-to-one imaging lens, the 70-mm film transport system, and the camera housing) was left unchanged. The CRT electronics and film-tension servos were completely redesigned using integrated circuit technology. The power requirement was thus reduced and this allowed the use of smaller and more compact low-voltage supplies than were used before. By locating certain compact circuit modules in the recorder, it was possible to eliminate some equipment racks. As a result of these changes, the recorder package weight was reduced by 145 lbs. A block diagram of the recorder electronics is shown in Figure 13.

5.1 RECORDING PROCESS

The radar data recording is accomplished by imaging an intensity-modulated single-line CRT trace onto photographic film which is moved continuously by means of the film transport system at about 10 mm per second. The film used is 70 mm-wide Kodak Microfile on 100-foot reels. The CRT line scan is divided into two portions, each of which records a 37μsec interval that corresponds to about a three-mile swath of imaged terrain. The recorded signal width of each channel on the film is about 28 mm with a 0.25 mm separation of channels at the center of the film. The portion of the film exposed for each channel is determined by the control module which supplies triggers to start the sweep and to unblank the proper portions of the sweep.

The start time of the sweep (with respect to the transmitter pulse) has to be changed periodically in order to display identical terrain in each channel (see Fig. 2). This is because the first half of each display sweep is used for recording parallel-polarization information and the last half for cross-polarization information. Thus, the sweep start is triggered by pulse t_2 for parallel-polarized signals and by the earlier pulse t_4 for cross-polarized signals. The CM determines the sequence of events. In normal operation (Mode 4), after four pulses all four channels have been sampled and the recording sequence starts over.

5.2 REFERENCE VOLTAGES

Precise reference voltages are required to maintain a stable CRT trace and to provide proper operating voltages to all other components of the displays. The reference voltage

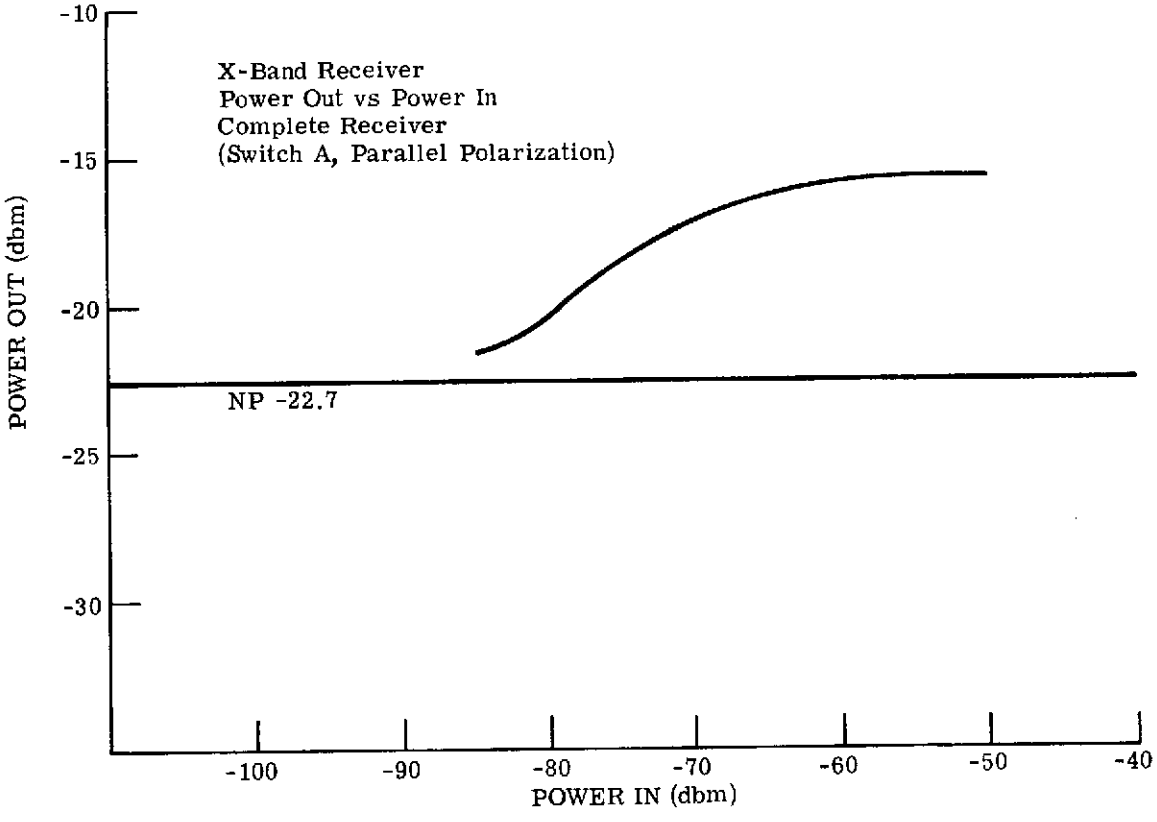

FIGURE 9. X-BAND RECEIVER GAIN-COMPRESSION CHARACTERISTIC (PARALLEL POLARIZATION)

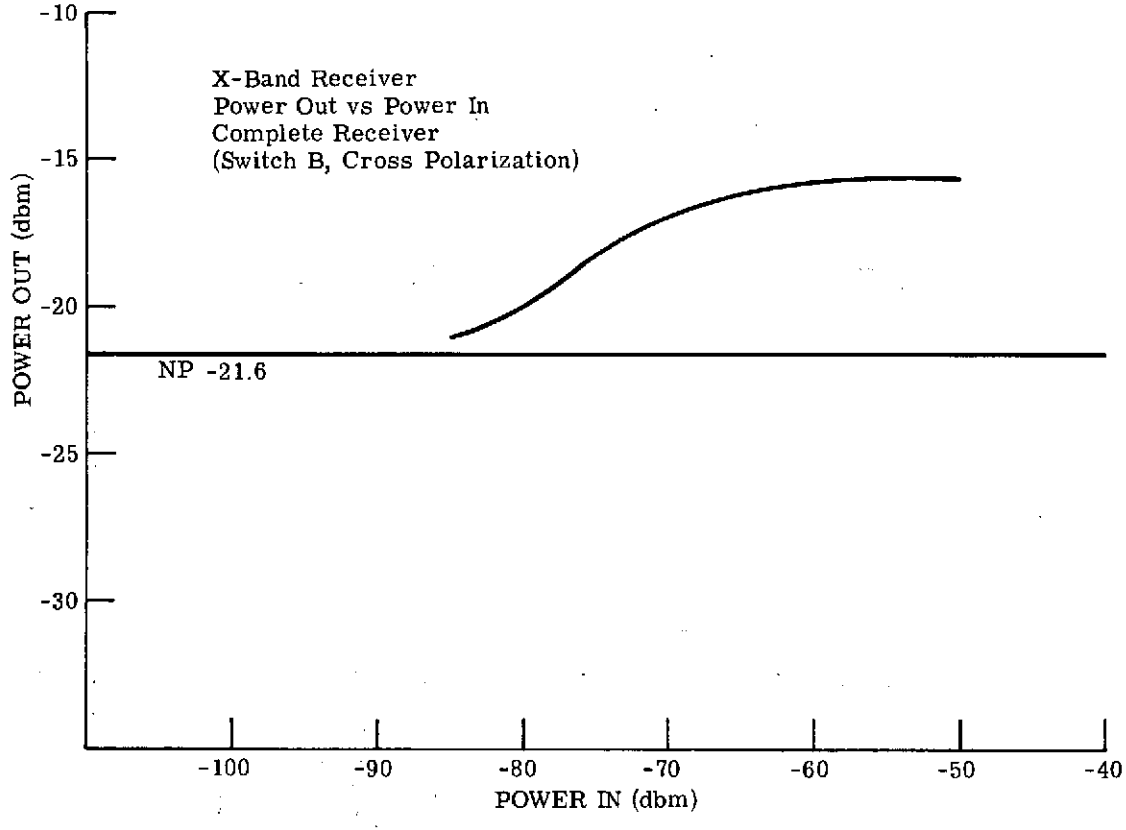

FIGURE 10. X-BAND RECEIVER GAIN-COMPRESSION CHARACTERISTIC (CROSS POLARIZATION)

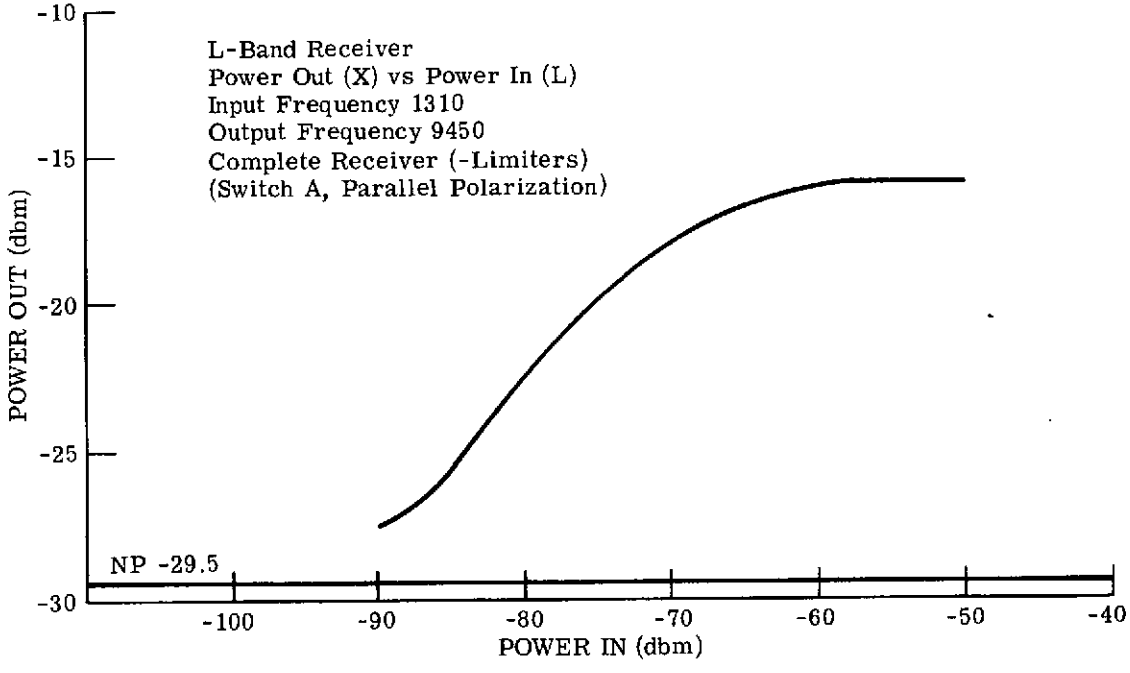

FIGURE 11. L-BAND RECEIVER GAIN-COMPRESSION CHARACTERISTIC (PARALLEL POLARIZATION)

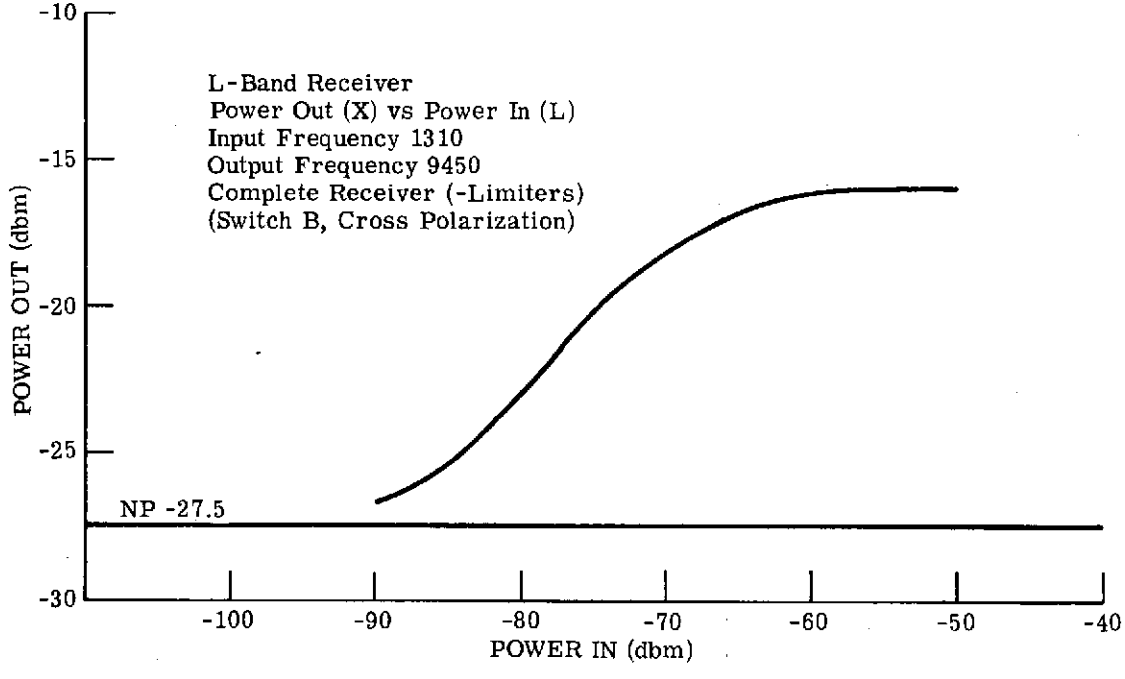

FIGURE 12. L-BAND RECEIVER GAIN-COMPRESSION CHARACTERISTIC (CROSS POLARIZATION)

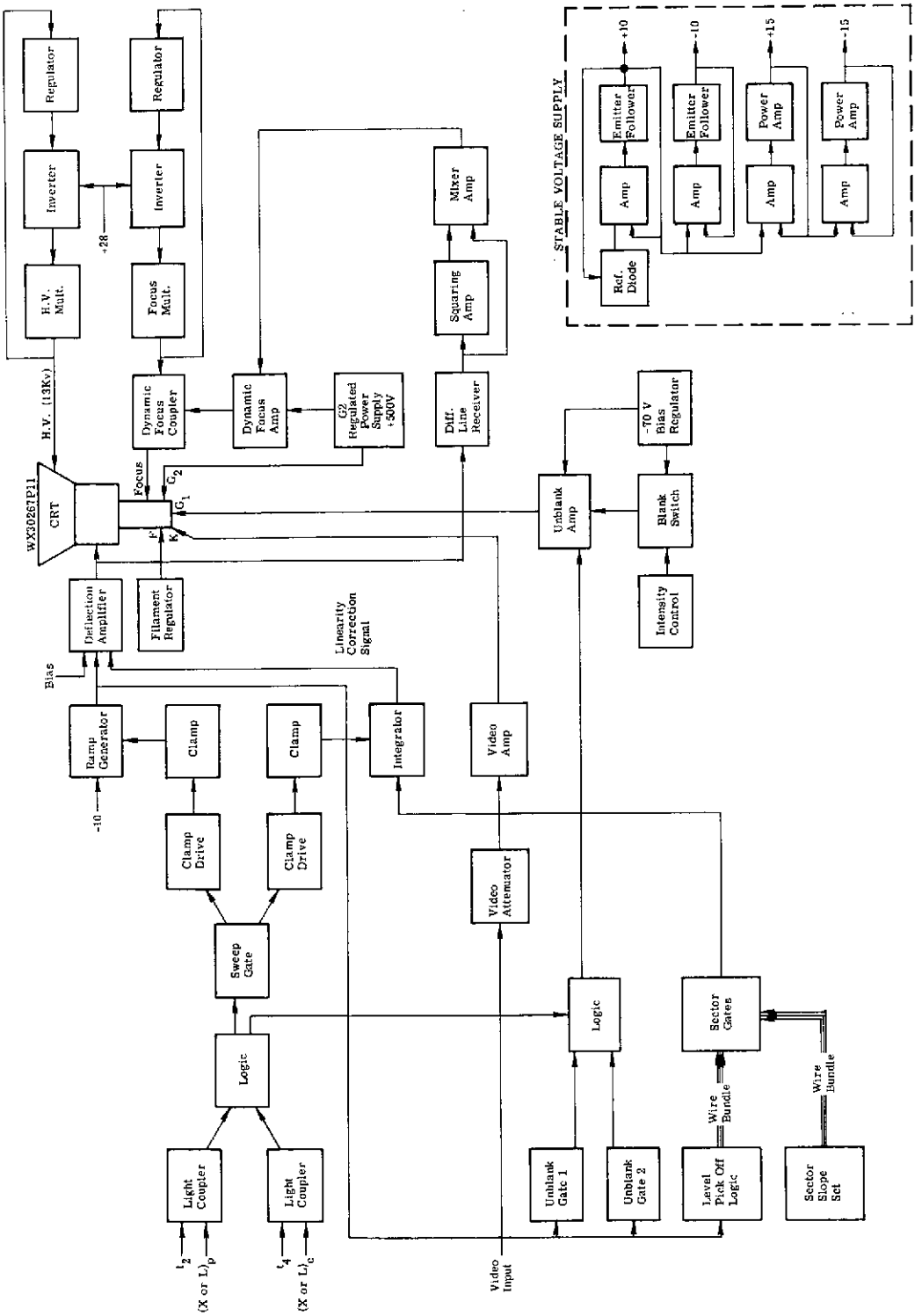

FIGURE 13. RECORDER ELECTRONICS BLOCK DIAGRAM

regulator circuitry provides precision ±10 V and ±15 V power and is shown in Figure 14. A reference Zener diode with a temperature stability of 5 ppm is used (upper left). The circuit is configured to take maximum advantage of operational amplifier technology, and all voltage-determining resistors have a temperature coefficient of 3 ppm. The Zener reference circuit is trimmed for +10.000 V output. When this is done, the other output reference voltages are also within one-tenth of one percent of their nominal values.

The supply voltage to the regulator circuit is ±20 V which may be varied down to ±16.7 V with less than a 0.001 V change in any of the outputs. Load-current variation from no-load to full-load causes the output voltages to change less than 0.001 volt.

Temperature tests performed by spraying liquid coolant on the circuit components show the reference Zener to be the most sensitive component on this circuit board by a factor of at least 3:1.

Another feature that has been provided in the design of the reference voltage regulator circuitry is protection from short circuits of any of the output voltages.

5.3 SWEEP GENERATOR

The sweep ramp generator circuitry shown in Figure 15 produces a sweep gate, a linear sweep, and a CRT unblank signal. The selected trigger (t_2 or t_4) operates a monostable multivibrator which produces the sweep gate signal. This signal is used in the unblank logic circuit and is also buffered in a level shifter to drive eight field-effect transistor (FET) switches in the linearity correction circuit and one here in the sweep circuit. The latter FET switch, located at the lower left in Figure 15, is connected across an integrating capacitor and an operational amplifier in order to generate a linear sawtooth voltage of 80μsec duration following each input trigger. This sweep signal is fed to the unblank logic circuit as well as (via an output terminal) to the deflection amplifier and the linearity correction circuit.

The unblank circuit utilizes two level sensors in conjunction with the sweep ramp. One of the resulting unblank signals starts at 4μsec after the sweep start and stops at 41μsec. The second unblank signal runs from 41.5 to 78.5μsec. The initial 4μsec at the beginning of the sweep is provided to allow for settling of the deflection system transients. The two unblank signals are gated with the CM mode signals (X_C, L_C, X_P, and L_P), combined, and fed to the CRT unblank output pin.

The CRT deflection amplifier shown in Figure 16 consists of an input amplifier and a power stage. The power stage has two complementary power transistors operating in Class B. There is local feedback around this stage which reduces the deadband, controls the gain, and flattens the frequency response. Its output voltage range is ±18 V and it typically delivers ±2.25 A. The deflection yoke inductance is 120 μH.

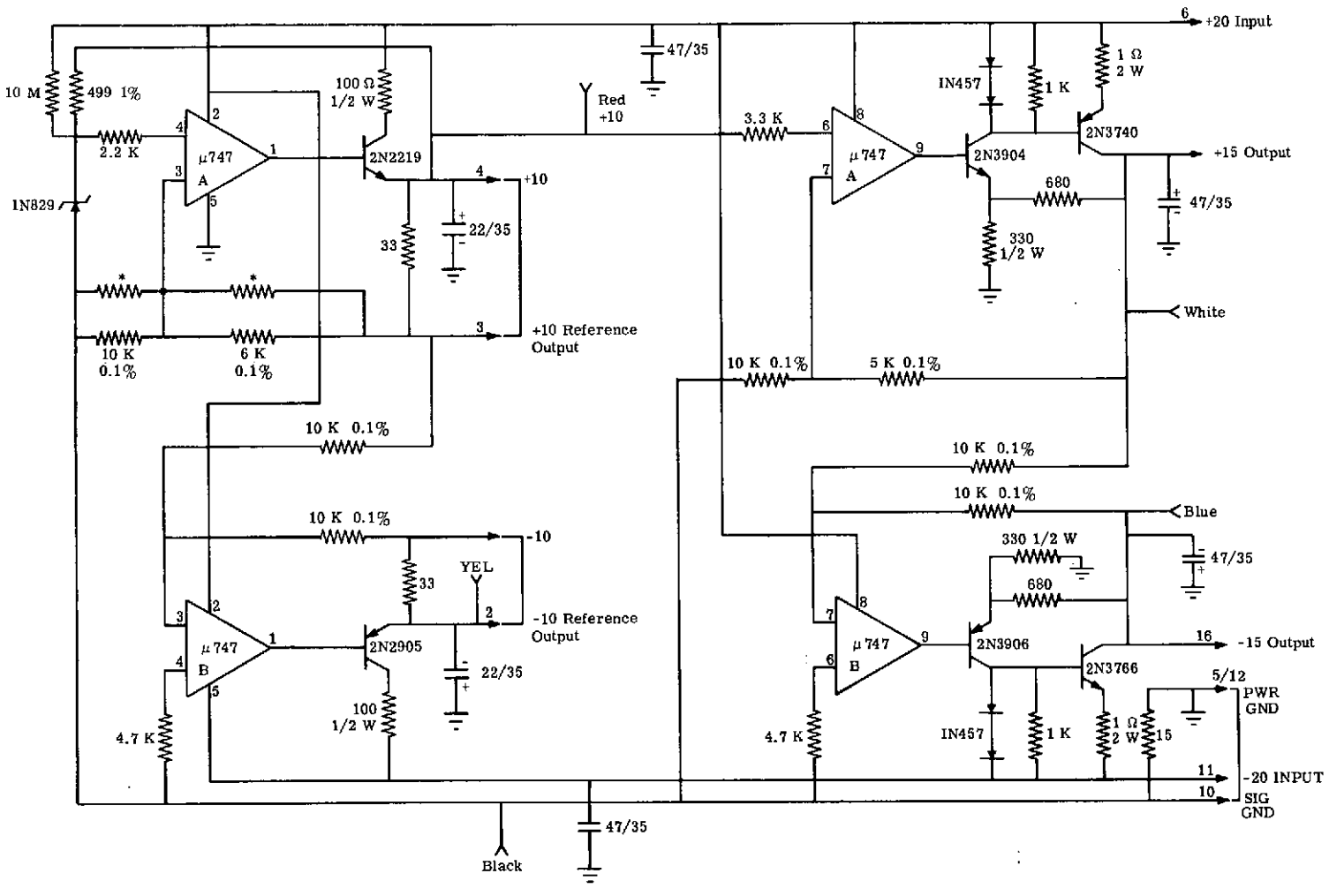

FIGURE 14. REFERENCE VOLTAGE REGULATOR

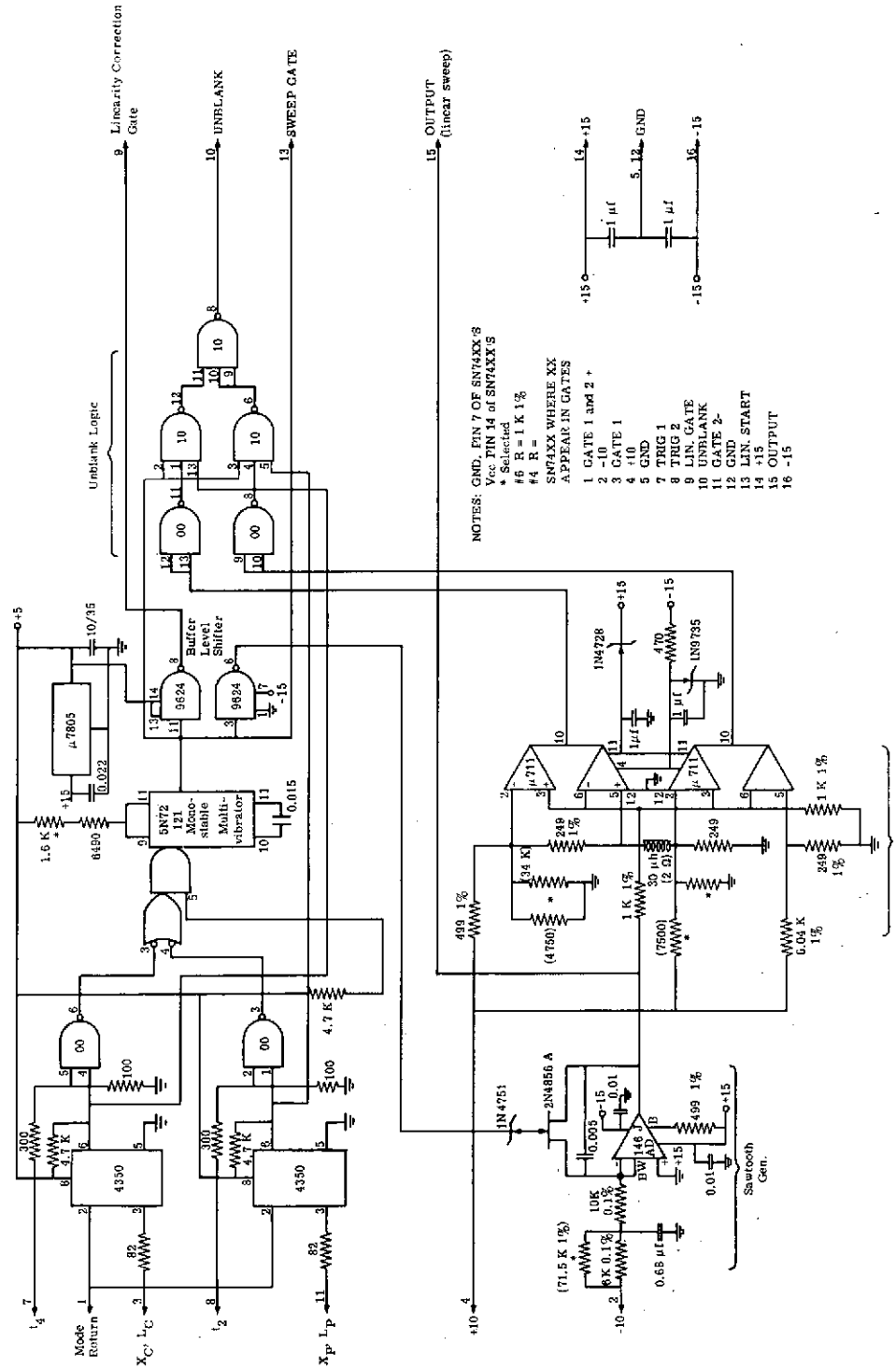

FIGURE 15. SWEEP GENERATOR

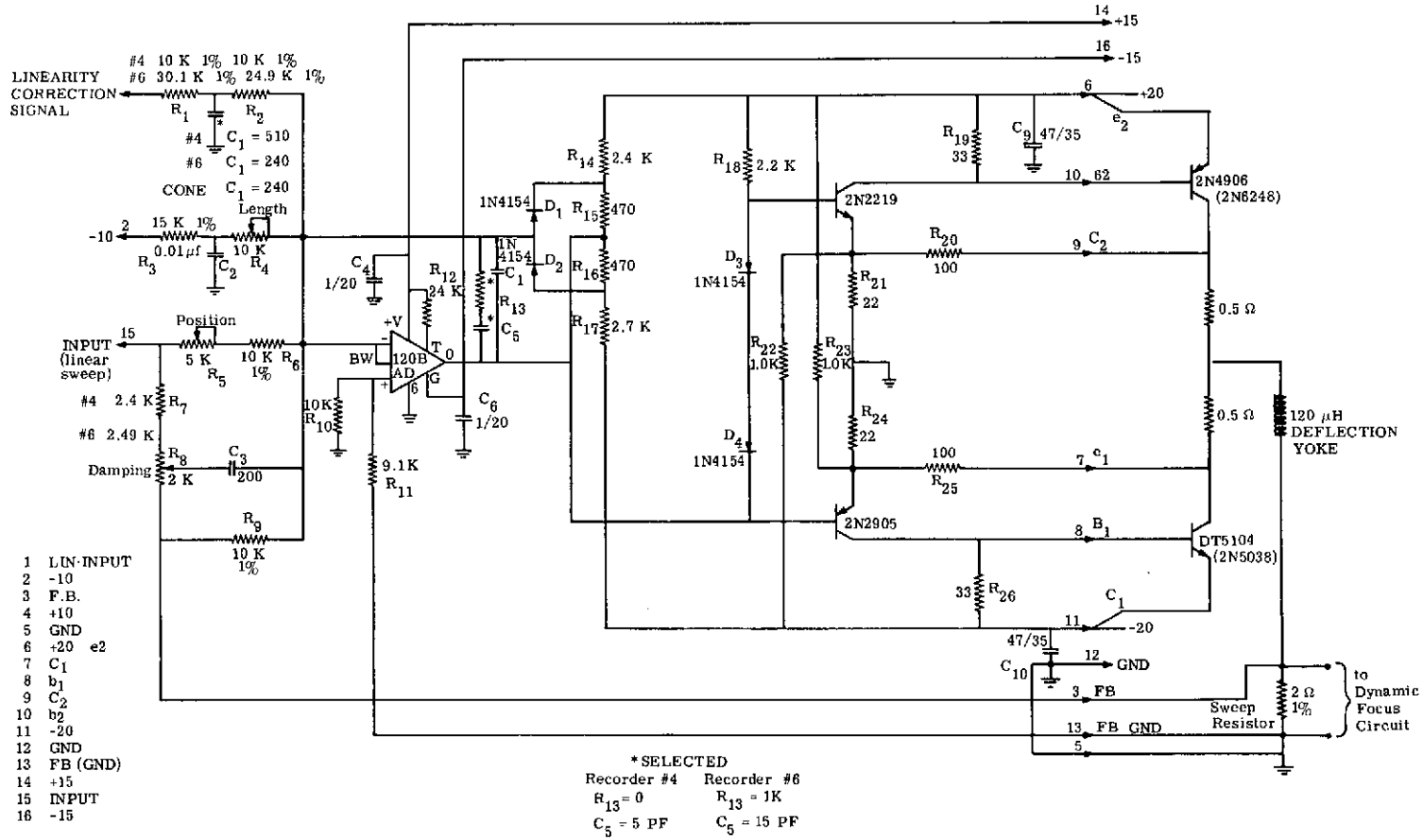

FIGURE 16. DEFLECTION AMPLIFIER

The deflection yoke current is made to follow the input signal by feeding back the voltage developed across a 2-Ω sweep resistor in series with the yoke. The input amplifier sums this feedback signal with the linear ramp voltage, the offset bias, and the linearity correction signal.

The input amplifier has a network (R_{13}, C_1, and C_5) between its input and output which reduces the high-frequency gain and stops very-high-frequency oscillation in the loop. There is also a yoke-damping network (R_7, R_8, and C_3) in the input circuit of the input amplifier. Proper adjustment of R_8 gives optimum coil damping. Two other adjustments are located in the input circuit. One (R_5) sets the start position of the CRT trace, and the other (R_4) sets the trace length.

5.4 LINEARITY CORRECTION

A linear current sawtooth in the yoke does not produce a linear sweep, because of the internal geometry of the CRT and the deflection sensitivity of the yoke. When these two factors are combined, the deflection current required for a linear sweep can be expressed as:

$$I = \frac{K\frac{x}{R}}{\sqrt{1 + \left(\frac{x}{R}\right)^2}}$$

where K is a constant

x is the CRT spot position measured from the center of the CRT face

R is the distance from the deflection center to the screen

$\tan^{-1}\frac{x}{R}$ is the deflection angle

The departure from a truly linear sweep is indicated by the denominator of this equation. This error factor increases with deflection angle and represents an increase in deflection system gain as the input deflection current increases. This error could be removed by modifying the gain of the deflection amplifier using a voltage proportional to the square of the linear sweep signal voltage. Because of the difficulty in stabilizing variable-gain circuits over the expected temperature variation, this method was not used.

An alternative method of linearizing the CRT sweeps was chosen which is more stable and easier to adjust. This method utilizes a correction voltage waveform added to the linear sweep waveform. An eight-segment, straight-line approximation to the theoretically-required correction waveform is used.

The deflection current equation can be rearranged to show the correction waveform as an addition to the initial ramp:

$$\frac{I}{K} = \frac{x}{R} + \frac{x}{R}\left[\frac{1 - \sqrt{1 + \left(\frac{x}{R}\right)^2}}{\sqrt{1 + \left(\frac{x}{R}\right)^2}}\right]$$

The second term is the ideal correction waveform. In practice, the linearity-correction waveform will also include residual nonlinear terms which are peculiar to the yoke and CRT assembly. The waveform used resembles one cycle of a sine wave.

Figure 17 shows the linearity correction circuitry. The input signal to the circuit is the linear sweep signal. Seven voltage levels are picked off of the sweep signal by high-speed operational amplifiers used as level detectors. The output of each operational amp. is combined with a signal from its adjacent one to form a gating signal for each straight-line segment. The segment slope is controlled by a potentiometer which is switched into the output integrator by the gate signals.

The integrator is clamped during sweep reset time, and this causes the output to return to zero volts at the beginning of each cycle. For one of the recorders, the eight segments of the linearity correction waveform are evenly spaced across the trace. For the other recorder, the pickoff voltages are set to produce short segments near the edges of the trace and long segments in the middle; this pattern was found to give better linearizing performance in this case. The output correction signal is sent to the deflection amplifier where it is combined with the linear sweep signal.

FET capacitance is troublesome in that it causes switching transients. Operating the FET switches in the shunt mode greatly reduces this problem.

Alignment of the linearity corrector is accomplished by the use of a CW intensity-modulation signal which is coherent with the trigger. A photographic film grating is placed over the CRT faceplate and the intensity-modulated trace is viewed through it. The beat pattern between the film grating and the modulated trace indicates departure from sweep linearity. First, the trace position and length are carefully adjusted with the linearity circuit card removed. The trace is adjusted to show two sections of zero beat pattern in the first and last quarters of the trace. This is done so that when the adjustments are finished, the trace length will be correct. Then, the linearity correction card is replaced and the segments are adjusted. Beginning with the start of the trace, each segment potentiometer is adjusted in turn for no beats. Slight interaction takes place between successive adjustments, so the adjustments are repeated a second time to optimize performance. The damping adjustment on the deflection amplifier is useful to obtain good sweep start linearity.

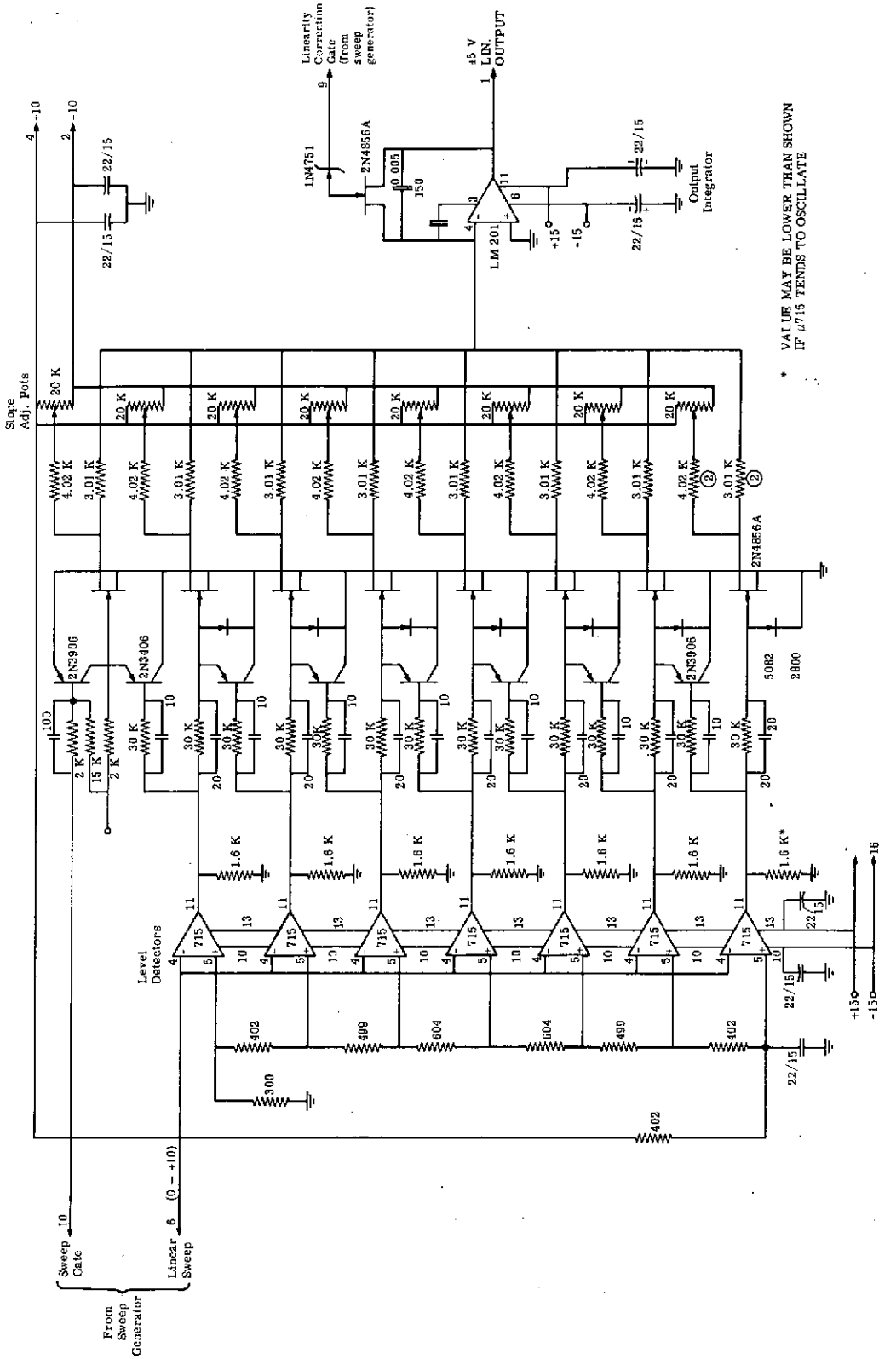

FIGURE 17. LINEARITY CORRECTOR

5.5 UNBLANKING AND DYNAMIC FOCUS

The unblanking amplifier and the dynamic focus parabola generator are mounted on the same circuit board. These circuits are shown in Figure 18.

The unblanking amplifier combines the unblanking signal with the exposure voltage from the brightness control. The unblanking signal causes a current-source amplifier to pull the CRT grid positive from -70 V until it is clamped by a diode at the output of the exposure amplifier. The exposure amplifier maintains its output one diode drop more negative than the exposure voltage, which compensates for the drop in the clamp diode. The rise and fall time of the unblanking pulse is about 1.0μsec.

The CRTs used in the recorders require a focus power supply of about 4300 V. The exact focus voltage required is a parabolic function of the spot position along the trace. This is accomplished by superimposing upon the DC focus voltage a parabolic waveform of about 160 V p-p, with the higher voltage occurring at the edges of the trace.

The dynamic focus waveform is generated from the deflection yoke current (see Fig. 18). The voltage across the sweep resistor (in series with the deflection yoke) is amplified to a suitable level and fed to a transconductance analog multiplier which forms the parabolic waveform. The focus parabola output has an amplitude of about 8 V p-p.

The circuit was designed to avoid interaction between adjustments. The focus supply sets the focus at the center of the trace and the parabola amplitude adjustment determines the focus at the leading edge. A sawtooth waveform is added to the last half of the parabola; its amplitude is adjusted to optimize the focus at the trailing edge of the trace.

The dynamic focus waveform is fed to another amplifier in the focus power supply package, shown in Figure 19. This parabola amplifier is powered by the +500 V supply and produces an output waveform whose amplitude is about 160 V p-p. The amplifier has a differential input followed by a high voltage transistor and a feedback network. The 100 K feedback resistor loads down the output transistor and keeps the output voltage below 250 V. After final amplification, the waveform is capacitively coupled to the CRT focus electrode. The parabola is also coupled to the output of the focus voltage supply and a set of diodes is used to DC-restore the center of the parabola to the focus supply voltage.

The focus power supply shown in Figure 19 consists of a high-voltage regulator, a transistor inverter, a high-voltage multiplier, and an output coupling network. The low-voltage input to the inverter is controlled as follows: Connected to the high-voltage output is a highly stable, high-resistance feedback resistor whose current is summed with a reference Zener diode voltage to form an error signal. This error signal controls the drive to the inverter. The output voltage is set to about 4300 V in the feedback control.

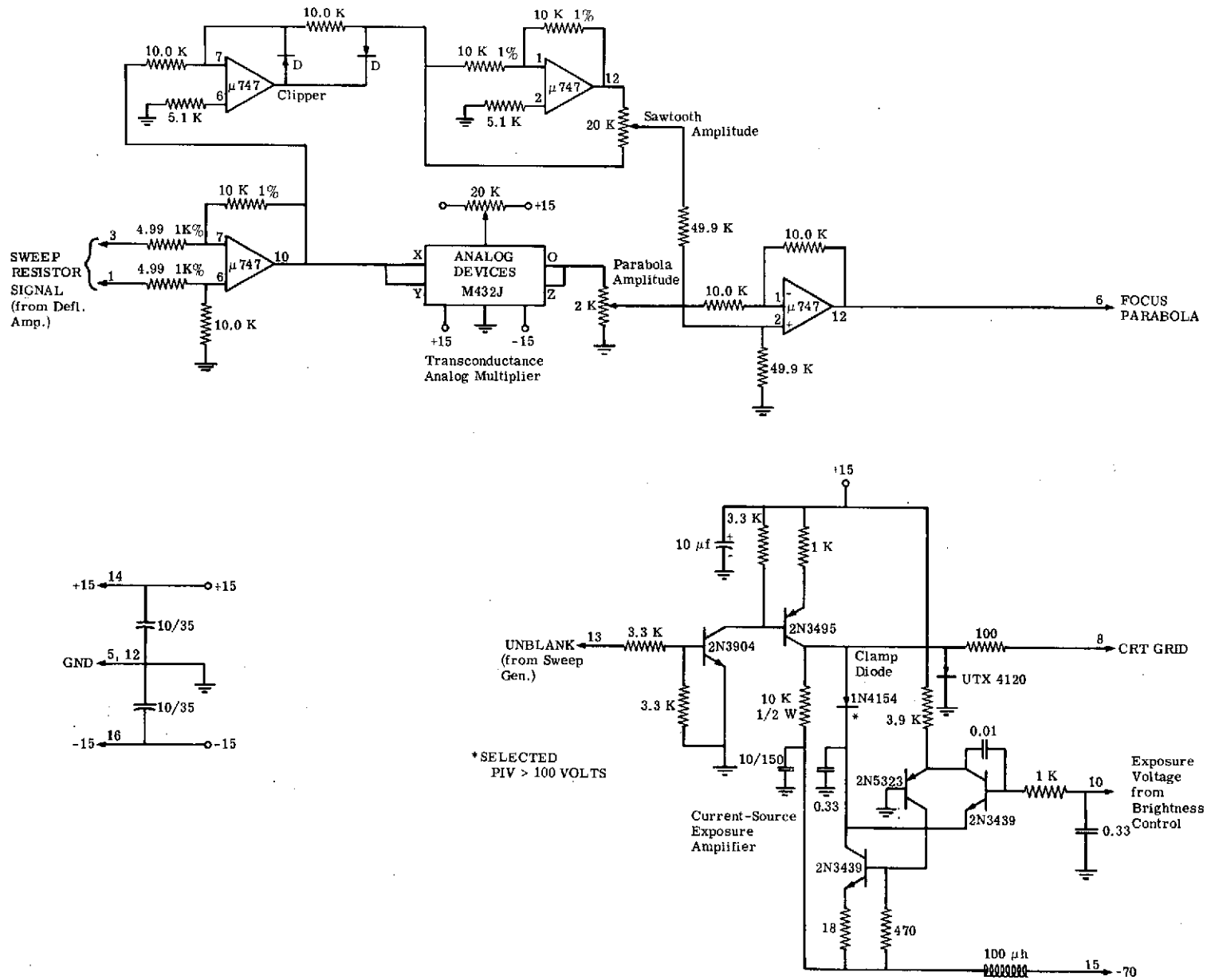

FIGURE 18. DYNAMIC FOCUS AND UNBLANKING CIRCUITS

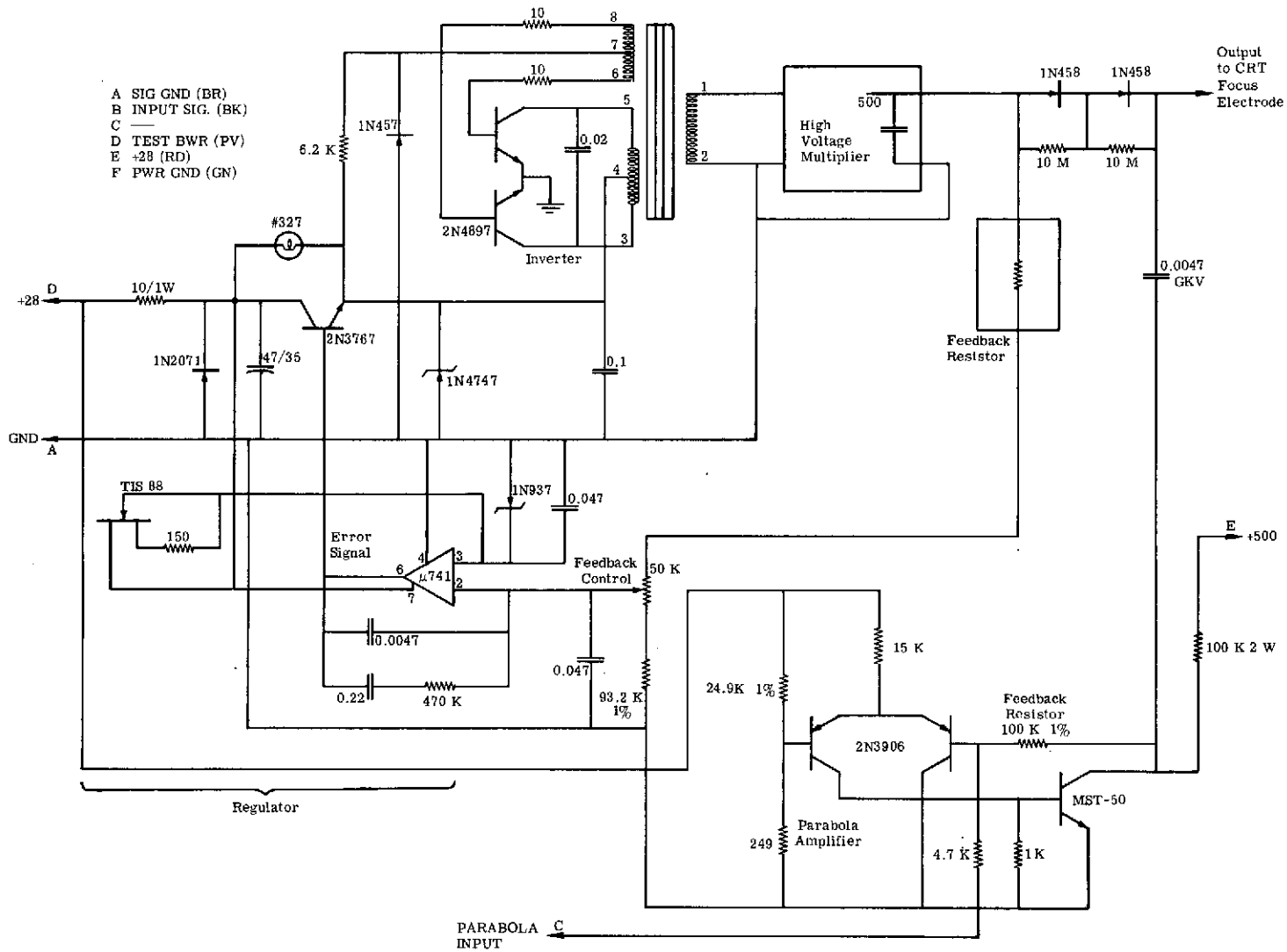

FIGURE 19. FOCUS VOLTAGE SUPPLY

5.6 ANODE VOLTAGE

The anode voltage supply is similar to the focus voltage supply shown in Figure 19. The low-voltage input to the inverter is controlled by a similar feedback arrangement in order to regulate the anode voltage. A lamp is placed in parallel with the inverter-driver transistor to indicate proper operation of the supply; the lamp is dim for normal operation. The supply's output voltage is set at 12,000 V.

5.7 CRT RESOLUTION

One of the recorders (No. 6) has a CRT whose resolution is better than average. Its spot size at the center of the trace is 0.00059 inches. (These tubes usually have about 0.00063-inch diameter spots and their specification calls for a maximum of 0.00065 inch.) When this tube is properly focused, a 74 line-pair per mm test pattern on the faceplate can be observed anywhere along the trace distinct enough to be counted. The CRT in the other recorder (No. 4) is an older tube and shows poorer resolution. A 37 line-pair per mm pattern can be observed easily on the No. 4 faceplate.

5.8 RECORDING LENSES

The lenses used in the recorders are a special design by the Perkin-Elmer Corporation for use in CRT recording. They were designed when the recorders were originally built in 1964. Each lens has an f-number of 2.8 and was designed for 2:1 demagnification. The distance between the object and the front lens surface is 12.254 in., and the distance between the image and the back lens surface is 6.054 in.; the overall distance from object to image is 23.291 in. The maximum usable trace length on the CRT is 108 mm, and the image on film is 54 mm long across both channels.

6
DATA PROCESSING

After photographic development, the four channels of recorded radar data are used to produce four output image films. The output images are obtained with two-dimensional pulse-compression on the recorded signals in an optical data processor. Different processor configurations are used for L-band and X-band.

The two X-band channels are processed by a commonly-used processing technique which employs a tilted-plane decoupled mode. This type of processor has been extensively described in the optical processing literature (e.g., Ref. 2).

The azimuth-to-range dimension aspect ratio is about 13.7:1 as recorded on the X-band data-storage film. The azimuth telescope is therefore set for a demagnification of 13.7 in order to produce equal scale factors in the output image. The limiting apertures at the frequency plane are adjusted to limit the signal passband in both dimensions to values commensurate with the image resolution. This aperturing is equivalent to filtering and serves to reduce extraneous noise while maintaining image resolution. The output imagery at the output plane of the data processor is a two-dimensional array of optical image components with a large intensity range.

The large dynamic range of the output image is strikingly visible to the human eye, but is too great to record linearly on photographic emulsion. The X-band radar imagery is recorded on Kodak #3414 film developed with D-76 developer (diluted 4:1) for 10 minutes. This low-contrast combination was chosen along with a convenient exposure level to minimize photographic blooming of very bright image components while still producing visible imagery of weak components such as lightly-reflecting terrain surfaces.

In processing to obtain the L-band imagery, a tilted cylinder optical-processor configuration is used (Ref. 1). The arrangement of the optical elements is shown in Figure 20. In the range dimension, lenses L_1, L_2, L_5, and L_6 operate to form an image at the output plane P_3 which is magnified 1.56 times relative to the input plane P_1. In the azimuth dimension, lenses L_2 and L_3 form a tilted-azimuth-plane image at plane P_2 which is demagnified 18.67 times relative to the input plane. The tilt of lens L_4 is adjusted to match the tilt of P_2. Then, L_4 and L_6 reimage plane P_2 at the output plane magnified 5.6 times, and the overall azimuth demagnification is 3.33:1. Because the range dimension is magnified 1.56 ×, the scale ratio is changed by a factor of $1.56 \times 3.33 = 5.2$, which is the azimuth-to-range aspect ratio on the L-band signal-storage film. This makes the output image scales equal in range and cross-range.

The L-band radar imagery, like the X-band, has a large dynamic range, and a choice of films must be made to produce an output image film with visible "ground painting" and yet without excessive blooming of bright-target images. The film chosen is Kodak Panatomic-X developed in D-76 developer for six minutes.

7
NAVIGATION AND MOTION COMPENSATION

7.1 REQUIRED FUNCTIONS

The airborne imaging radar uses the synthetic aperture technique to provide fine resolution in the cross-range (azimuth) direction. A synthetic aperture radar requires auxiliary systems which use inertial references to accomplish four different functions.

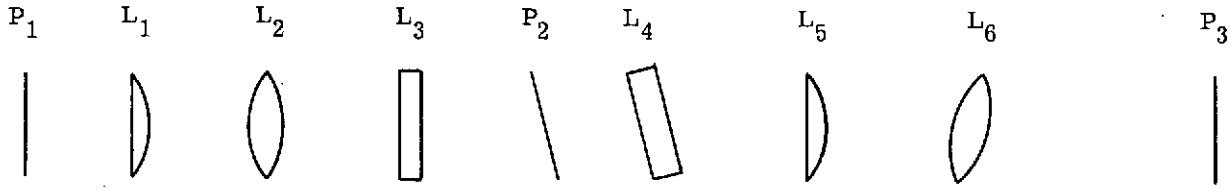

P_1 Input Plane
P_2 Tilted Azimuth Plane
P_3 Output Plane

L_1 560 mm Cylinder
L_2 560 mm Sphere
L_3 30 mm Cylinder
L_4 100 mm Cylinder
L_5 359 mm Cylinder
L_6 560 mm Sphere

FIGURE 20. TILTED-LENS OPTICAL PROCESSOR

First, a desired track must be established and the aircraft must be guided along this path so that the radar beam scans over a particular strip of terrain. This is done by establishing a straight line at the altitude of the aircraft based on the desired terrain swath and the operating range of the radar. An inertial navigation system in the aircraft is used to provide guidance signals for the aircraft's autopilot in order to navigate the aircraft along this line.

Second, the radar antenna must be stabilized to hold the radar beam perpendicular to the desired track and at the appropriate depression angle. The aircraft forward velocity then scans the beam along the desired terrain swath. Angular orientation signals are taken from the inertial platform to control the antenna servo so that the antenna maintains its proper orientation as the aircraft maneuvers in following the desired track.

A third function requiring inertial sensing is that of accurately correcting the radar echo signal phase for residual range-direction displacement of the radar antenna from the desired flight path. This is done by taking acceleration signals from the inertial platform, computing the component of motion along the line of sight to the target area, and shifting the phase of the radar signals (prior to recording) by an amount sufficient to cancel the motion phase shifts.

A fourth function is synchronizing the radar offset frequency, the pulse repetition frequency, and film speed of the radar recorders to the aircraft along-track velocity. Along-track velocity signals are taken from the inertial platform and applied to the offset frequency circuitry, the local time base, and the film drive servos.

7.2 DOPPLER-INERTIAL SYSTEM

The above functions had been provided in ERIM's C-46 aircraft by an inertial platform coupled to a Doppler navigation radar. Antenna orientation was controlled directly by the inertial platform. Navigation of the aircraft was accomplished by the use of Doppler navigation system drift-angle information. The difference between the Doppler track angle and the antenna angle was used as a navigation error signal to guide the aircraft by means of a navigation gyro and the autopilot. In this way, the aircraft was stabilized in level flight and guided in a direction parallel to the desired track. Aircraft velocity information was obtained from the Doppler navigation system, and lateral acceleration information from accelerometers mounted on the inertial platform. This system, which had been used for several years, allowed lateral displacement from the desired track although it did maintain the aircraft flight direction parallel to the desired track.

7.3 ALL-INERTIAL SYSTEM

A modern all-inertial navigation system (INS) was believed capable of providing all of the required stabilization and navigation signals for the functions listed in Section 7.1. An all-inertial system is typically smaller, lighter, and lower-powered than the older Doppler-inertial

system. While the INS had not been experimentally proven in this application, analysis of one such system, the LTN-51, indicated that it probably would perform adequately without extensive programming modifications. One type of navigation of which the LTN-51 is capable makes use of indicated displacement from a desired great circle track in order to guide the aircraft along the actual desired path rather than merely parallel to it. This appeared to be an attractive feature that could improve radar performance. On the basis of this analysis, then, the LTN-51 was selected for use in the aircraft with the dual-band imaging radar.

In changing to this new commercial navigation system, all of the radar system connections to the existing Doppler-inertial system had to be removed and new ones designed and constructed. A standard LTN-51 was used along with a modified operational computer program. In addition to the features of the standard LTN-51 program, this modified program provides for (1) either roll or yaw steering (selectable by discrete control), (2) the insertion of steering-equation gain constants via the LTN-51 control/display unit, and (3) specialized outputs.

A diagram showing the coupling of the inertial system to the radar and the aircraft is presented in Figure 21. The navigation loop connecting the INS with the autopilot and the airframe appears at the top. The antenna stabilization loop is on the left. Film-speed and Doppler-frequency-offset control begin with an approximate along-track velocity signal V_T from the INS which supervises an accurate velocity computation based on the along-track acceleration A_T. The computed along-track velocity signal is fed to the radar to determine offset and pulse-repetition frequencies, and to the recorders to control film speed. The motion-compensation loop is located near the center of Figure 21. Acceleration signals from the INS are resolved, integrated, and applied to a phase shifter in the radar. The motion-compensation system is discussed in more detail in Section 7.4.

Three manual inputs are indicated. The autopilot sensitivity control is set to provide tight conformity of the aircraft to the desired track. The antenna offset control allows the antenna to be set precisely on the desired isodoppler line. The desired track and wander angle control is used to set in any desired track and to account for the inertial-platform wander angle. Since the platform is not constrained in azimuth and may be oriented at any angle, this control permits the velocity and acceleration signals that are taken from the platform to be resolved into along-track, across-track, and vertical components.

7.4 MOTION COMPENSATION

The synthetic aperture technique depends upon the predictable echo-signal phase histories which are produced as the radar antenna is transported along a straight-line path. As described above, a navigation system is provided to guide the aircraft along this straight line; but, despite this guidance, some displacements of the antenna from the desired track occur. Even

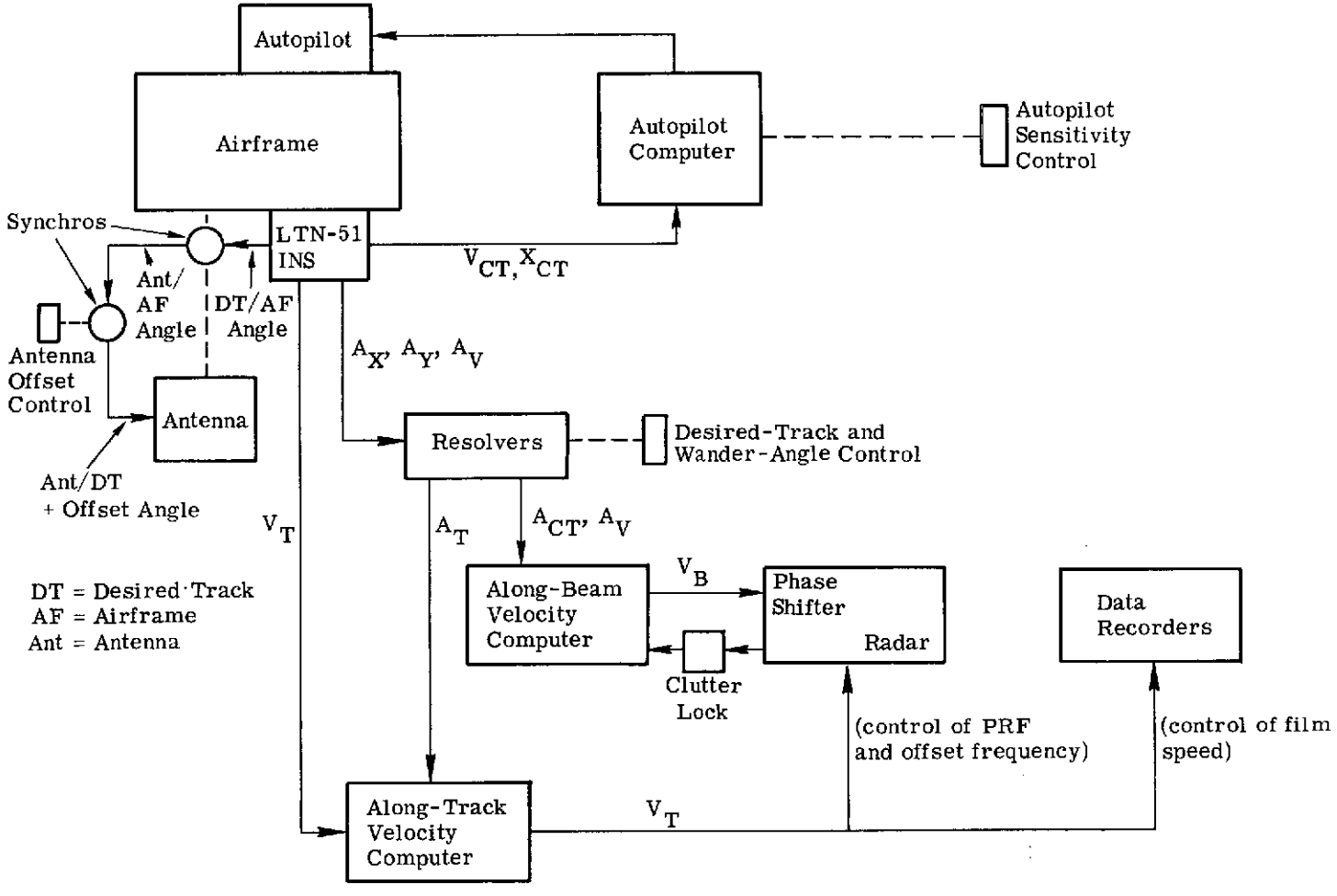

FIGURE 21. NAVIGATION AND MOTION COMPENSATION SYSTEM

small lateral displacements cause distortion of the quadratic phase rate that is utilized in the data processor to obtain fine-resolution imagery (Ref. 3). Therefore, a motion-compensation subsystem has been designed to apply "fine-grain" phase correction to the radar. This subsystem measures the motion inertially and shifts the phase of the radar signals just enough to cancel the motion-induced phase shifts; this phase correction is accomplished before the signals are recorded on the data storage films.

The block diagram of Figure 21 includes the complete motion-compensation system, while Figure 22 shows a portion of the resolvers block and the complete along-beam velocity computer block in more detail. The INS provides the three orthogonal acceleration component signals A_x, A_y, and A_V. The A_x and A_y components are resolved into the cross-track component A_{CT} by means of sin ϕ and cos ϕ, where ϕ is the angle between the desired beam orientation and the actual platform orientation. Then, the components of A_{CT} and A_V in the along-beam direction are computed by means of sin θ and cos θ, where θ is the depression angle. These two components are added together to form the total along-beam acceleration A_B. Finally, A_B is integrated in order to produce the along-beam velocity V_B. Signal V_B is fed to a phase shifter located in the radar's X10 Multiplier in order to shift the phase of the Offset STALO frequency (see Fig. 1). (Along-beam velocity is not computed directly from the velocity signals available in the INS because the lateral velocity is small compared to the forward velocity and, as a result, the computation would not be sufficiently accurate.)

As can be seen in Figure 21, the along-beam velocity computer is lightly damped by means of a loosely-coupled clutterlock feedback loop which senses the average Doppler frequency of the radar echoes. The clutterlock output signal is zero when the average echo-signal offset is correct. Also, a fail-safe feature makes this clutterlock signal zero when the echo signal level drops to zero. Care must be taken to keep the gain of the clutterlock loop low enough so that the loop does not add phase error by coupling circuit noise into the velocity computer.

While the beam-velocity computer has a loose frequency lock because of the clutterlock feedback loop, there is no phase-lock feedback loop. Phase compensation thus depends entirely upon computing instantaneous along-beam velocity and shifting the signal phase at a rate that matches the echo phase-rate from lateral motion. The correcting phase-rate must be accurately calibrated on the ground and cannot be recalibrated during flight. Any miscalibration will appear as incompletely-compensated signals and non-constant focus of the along-track dimension in the radar imagery.

The motion-compensation system for the dual-band radar uses two scale factors alternately as appropriate for the two radar wavelengths. This represents a fairly modest addition to the existing system, and was accomplished by the use of a switch (not shown) at the output

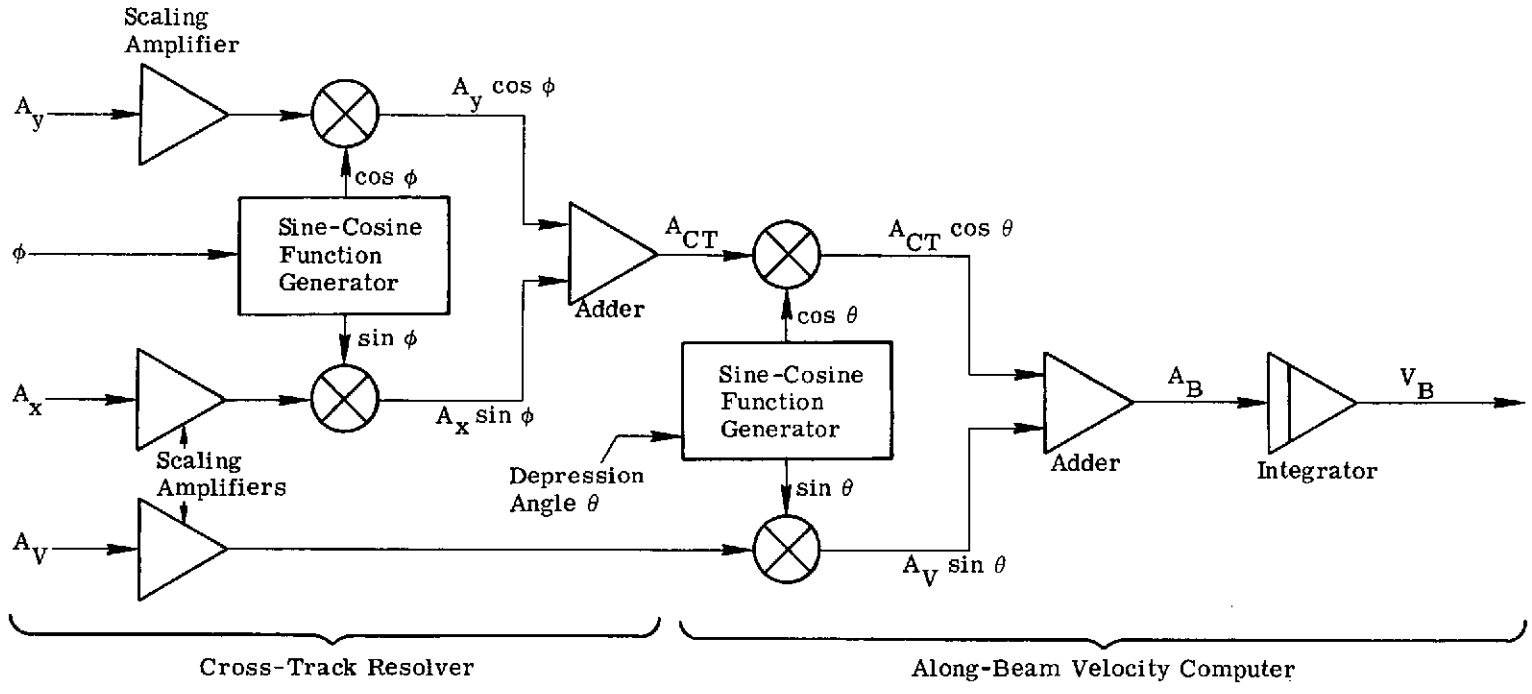

(ϕ = Angle between desired beam orientation and actual inertial platform orientation)

FIGURE 22. CROSS-TRACK RESOLVER AND ALONG-BEAM VELOCITY COMPUTER

of the beam-velocity computer. The switch is operated by the control module and applies different scale factors to the phase shifter in the radar. The control signals are indicated in Figure 3.

7.5 NAVIGATION AND MOTION-COMPENSATION FLIGHT TEST

A flight test was conducted in November 1972 (prior to the completion of the dual-band radar). In this flight, the LTN-51 provided autopilot supervision, antenna stabilization, and along-beam acceleration signals. The aircraft was guided along the desired flight path in a stable manner, but the quality of guidance was not accurately determined because of frequent unscheduled changes of flight path. The radar antenna appeared to be stabilized by the LTN-51 signals in terms of short-term variations, but the long-term performance was not entirely satisfactory. A large, slowly varying offset of the antenna from the zero-Doppler line has not been completely explained. The along-beam acceleration signals appeared to be adequate to compensate for lateral motion.

A subsequent test flight later in November 1972 indicated a continuing antenna orientation problem with large and variable misorientation of the antenna. Compensation of the radar data for lateral motion appeared good with light damping of the along-beam velocity computer by the clutterlock signal. The navigation accuracy appeared good; pass-to-pass displacements of the imaged swaths were only a small part of a swath width.

The LTN-51 system was rented again after the dual-frequency radar was installed in the aircraft. Test flights were made in March and April of 1973; these flights are discussed in Section 9.

8
INSTALLATION

The installation of the dual-band radar system in ERIM's C-46 aircraft was initially viewed as a minor part of the program. However, it was found to involve a very extensive alteration of the airborne equipment. Almost every component of the airborne radar system was removed from the aircraft for modification or replacement, and considerable modification of the cabling within the aircraft was required. Preparation of the items to be installed in the aircraft took longer than expected and the final installation was not completed before the termination of the contract period.

After the various components of the dual-band radar were physically installed in the aircraft and interconnecting cables were fabricated and installed, the entire system had to be checked out and modified to produce an operational imaging radar system. The initial

installation took about ten man-weeks, while the checkout and modification required about six additional man-weeks.

Three portions of the airborne system caused extension of the installation and checkout period. The first was the interfacing of the LTN-51 inertial navigation system (INS) with the autopilot; the second was associated with the four-channel antenna; and the third was related to synchronizing the A-scope monitor with each of the four channels.

The LTN-51 work has been covered in Section 7.5. A diagram of the principal units and their interconnections is shown in Figure 23.

The antenna used in the dual-band radar has four separate RF channels: X-band parallel-polarized, X-band cross-polarized, L-band parallel-polarized, and L-band cross-polarized. The addition of these multiple channels resulted in an antenna system which weighed 120 lbs mounted on a pedestal that had formerly held a 30 lb antenna. Not only was the multi-channel antenna heavy but its balance was so changed that the torque required to turn it in azimuth increased. During checkout, it was determined that an azimuth servo system with higher torque was needed, and a new shunt-wound dc servo motor-tachometer was installed. This new motor required a new servo amplifier to supply the required motor current. It was found that the new motor then had adequate torque to position the antenna with the required accuracy. The servo error signal and the gyro output signal are among the signals that are monitored continuously in flight by recording them on a multichannel oscillograph. These records indicate position errors of less than five arc-minutes in normal airborne operation.

The A-scope monitor synchronizing problem resulted from the available sync which triggers at the system PRF (nominally 8 kHz) while the video signals of any one channel occur at 1/4 this rate. The Control Module was modified to provide eight sync signals to select as A-scope triggers. They are shown in Table 4. In order to monitor a particular video channel, the sync selector is moved to Sync 1 (recorder unblanking) and the appropriate sync mode is chosen. If it is desired to display a transmitter channel, Sync 2 (BWO trigger) is selected along with the proper sync mode.

The transmitters and receivers with their large traveling-wave tubes and waveguide circuits (including stabilizing X-band cavities) were mounted in racks in the laboratory and installed in the aircraft without incident. Photographs of these racks are shown in Figures 24 and 25.

Final installation and checkout was completed in March of 1973. Subsequent flights have resulted in further shakedown and refinement of the entire imaging-radar system.

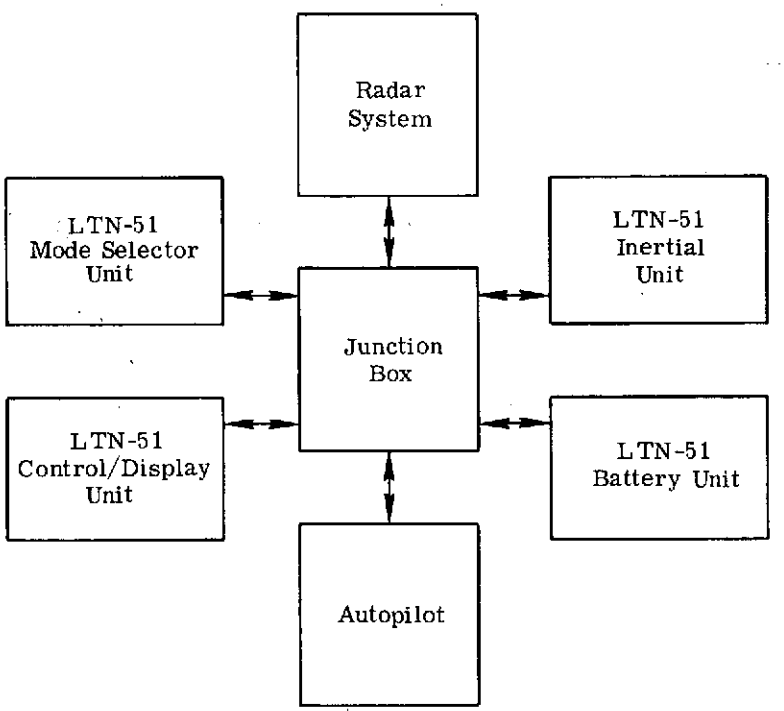

FIGURE 23. LTN-51 INERTIAL SYSTEM INTERCONNECTIONS

TABLE 4. A-SCOPE TRIGGER SYNC SIGNALS

Sync Mode	Sync 1 (Recorder Unblanking)	Sync 2 (BWO Trigger)
1	X-parallel	X-parallel
2	L-parallel	L-parallel
3	X-cross	X-cross
4	L-cross	L-cross

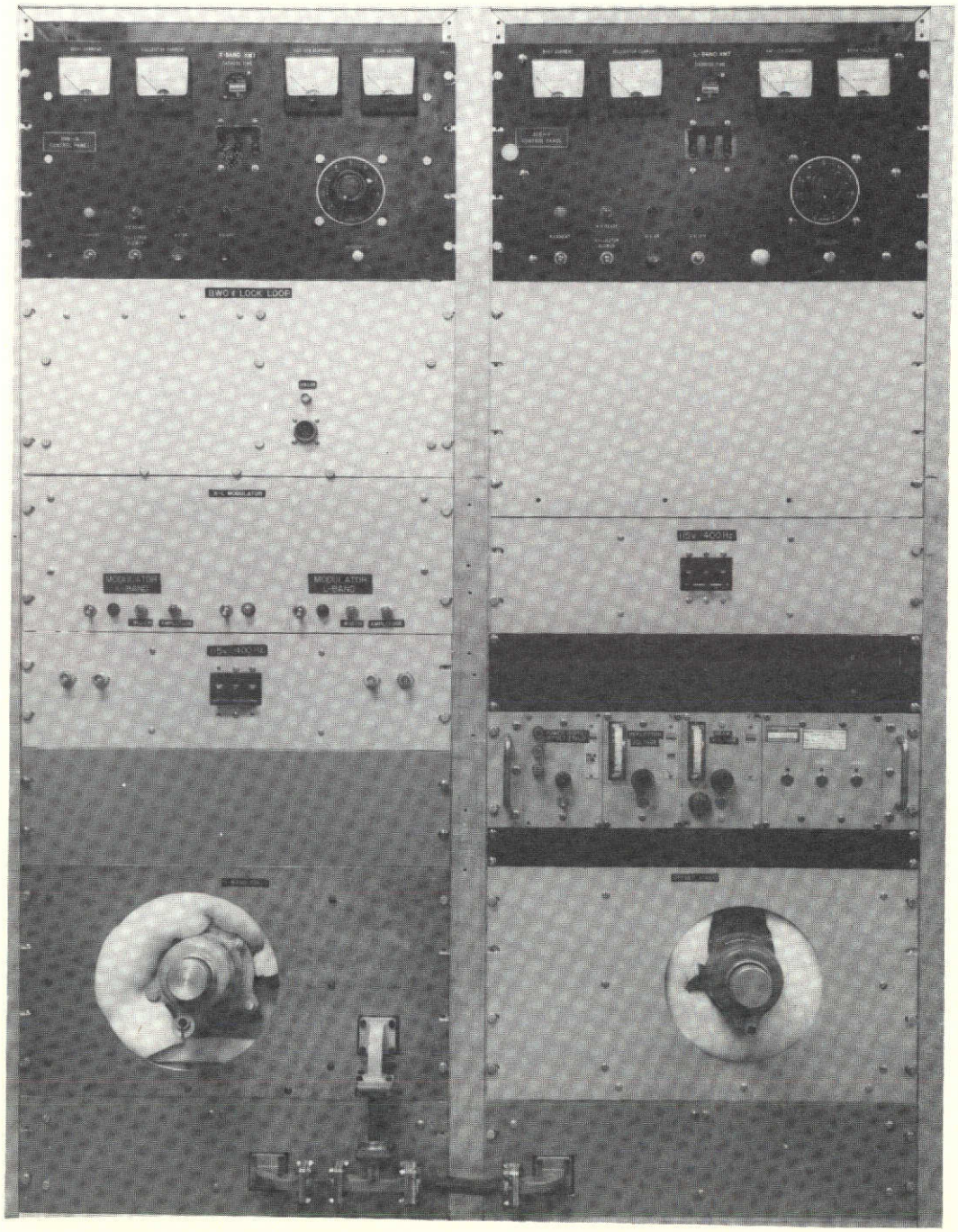

X-Band L-Band

FIGURE 24. TRANSMITTER-RECEIVER ELECTRONICS, FRONT VIEW

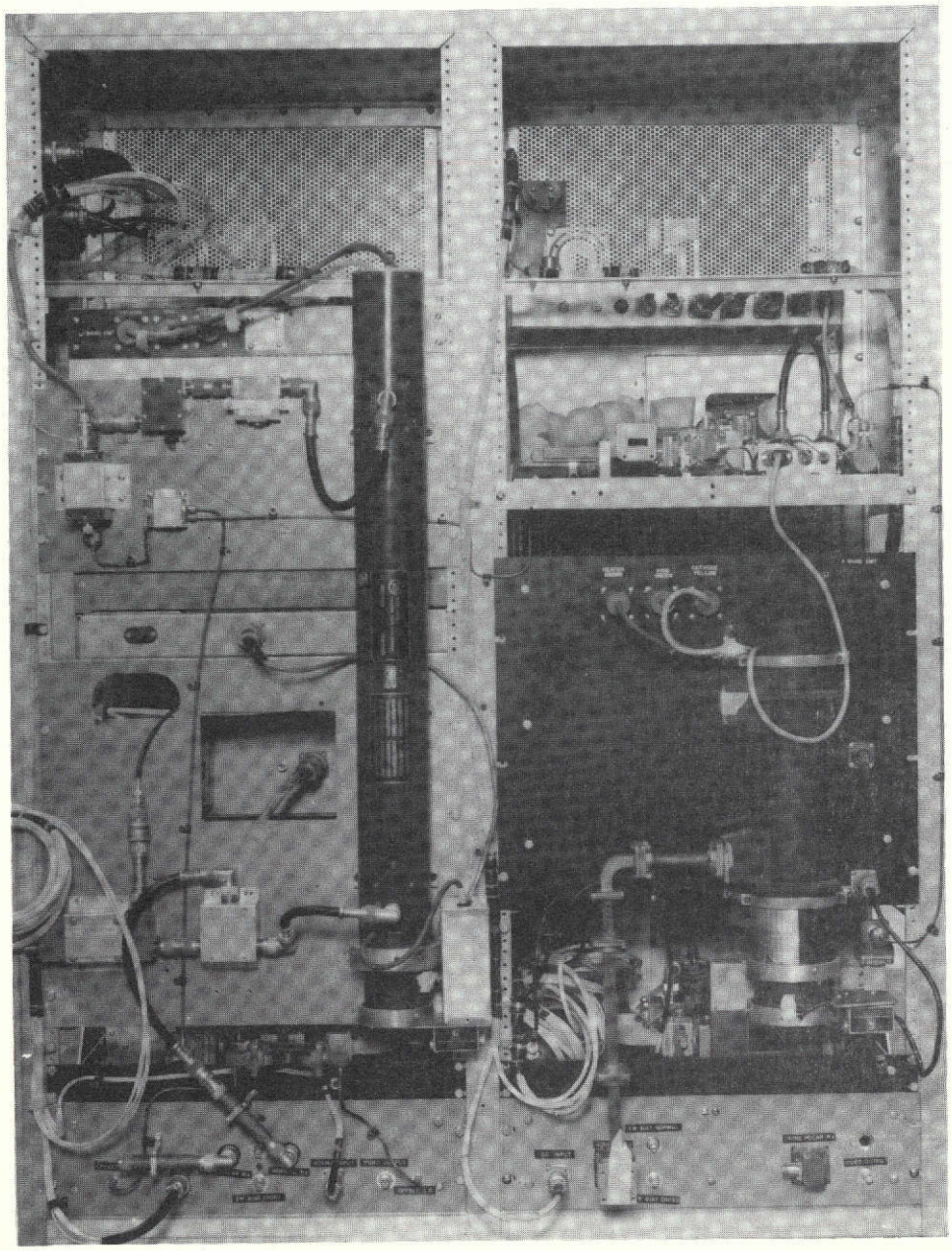

L-Band X-Band

FIGURE 25. TRANSMITTER-RECEIVER ELECTRONICS, REAR VIEW

9
FLIGHT TESTS

Three test flights were made with the entire dual-band radar system in March and April of 1973. The purpose of the first flight (on 21 March) was to allow adjustment of the clutter-lock feedback loop, the antenna offset angle, and the autopilot gains while airborne. It was intended also to obtain radar imagery of the terrain in order to demonstrate operation of all components and to assess the quality of the imagery produced by the multichannel system.

It was observed that the newly-constructed control module operated satisfactorily, although changing the range delay was found to be somewhat cumbersome.

The transmitters operated reliably throughout the entire flight. However, some malfunctioning was indicated by the appearance of the imagery. There were prominent sidelobes extending downrange quite visibly from all bright image components. This effect probably resulted from nonlinear frequency modulation of the BWO in generating the transmitter signal. Careful adjustment of the modulating ramp should clear up the image pulse shape.

Modulation sidebands were detectable only on the brightest image components. We concluded, therefore, that phase modulation of the radar signals by vibration in the aircraft was quite small.

The spectra of recorded signals on all four channels were severely banded, evidently caused by video mismatch in the receiving channels. (The third flight on 5 April 1973 produced signal films with greatly improved recorded signal spectra.)

The far-range portion of the imagery is faded because of misalignment of the radar antenna tilt and the delay used in the recorders. Although the vertical field patterns of the radar antennas have no cosecant-squared portion, the antennas can be tilted to provide a minimum of amplitude taper over the displayed swath.

One of the four recorder channels was improperly delayed and imaged a terrain swath displaced from the other three. (All four channels were closely coincident for the second flight on 28 March.)

Both signal films showed signs of non-uniform transport speed. There were slight striations resulting from momentary stops and some heavy stripes due to unscheduled long-duration stops. (This problem was eased on the second flight but was not completely cleared up until October 1973.)

The LTN-51 inertial navigation system provided only fair navigational accuracy. Repeated passes to image the same terrain swath resulted in displacements within about one mile most of the time. Some rotation of the aircraft track was observed, and some displacements greater than a mile occurred. These navigational errors may be due to inexperience in aligning the inertial system and inserting updating information.

The most troublesome aspect of the LTN-51 performance was its inability to orient the radar antenna stably with reference to the desired track. Bias errors, long-term drifts, and short-term instability were all observed. The antenna was misaligned by varying amounts up to about 3^{o}. This misalignment caused a large offset in the Doppler frequencies of the echo signals which could be compensated for only by setting (automatically or manually) a large bias into the along-beam velocity computer. This compensation held the Doppler frequencies within a workable bandwidth, but a large amount of range walk was left in all recorded signals, and data processing became more difficult than normal. The inertial platform rental period elapsed, and it was returned before the problems encountered with it could be fully analyzed. Additional study of the inertial system and its coupling to the radar is clearly required.

Phase correction of the recorded radar signals to compensate for lateral motions of the aircraft appeared to be satisfactory when damping of the velocity computer was sufficiently light. Although no exhaustive tests of the achieved resolution were performed, it was clear that the imagery was better focused with motion compensation than without it.

Clutterlock-damping of the motion compensation computer was only partially successful. Further adjustment of the circuit parameters is needed to optimize performance.

For all the system faults disclosed by this very limited test flight program, some simultaneous four-channel imagery was produced. It is quite recognizable terrain imagery and it shows both polarization and wavelength effects which may be exploited in the remote sensing of terrain features.

The second and third flights were made under separate sponsorship on 28 March and 5 April 1973 to obtain dual-band radar imagery of particular sections of terrain. Some imagery was utilized in a preliminary evaluation of the utility of dual-polarized, dual-frequency radar imagery in remote sensing. Examples of the four simultaneous images from the April flight are shown in Figure 26.

The imaged swath is located in Monroe County, Michigan and shows the Lake Erie shore with Stoney Point at the upper right and the mouth of Swan Creek near the top center. North is toward the left in this imagery. The area is only slightly above lake level and is used largely for agricultural purposes. Some of the land near the lake was flooded by high lake levels at the time that the area was imaged. Some lakeshore homes and cottages appear along the Lake Erie shore north (left) of Swan Creek and at Stoney Point. Along the lakeshore south (right) of Swan Creek, the Enrico Fermi generating station is under construction and two cooling towers can be seen. One is completed and shows a small image from its smooth front surface. It casts a shadow downrange toward the lake. The other tower, with only its low structural members in place, is imaged just north of the first one as a circle with no shadow. The difference in reflectivity of the terrain for the two radar wavelengths is quite noticeable.

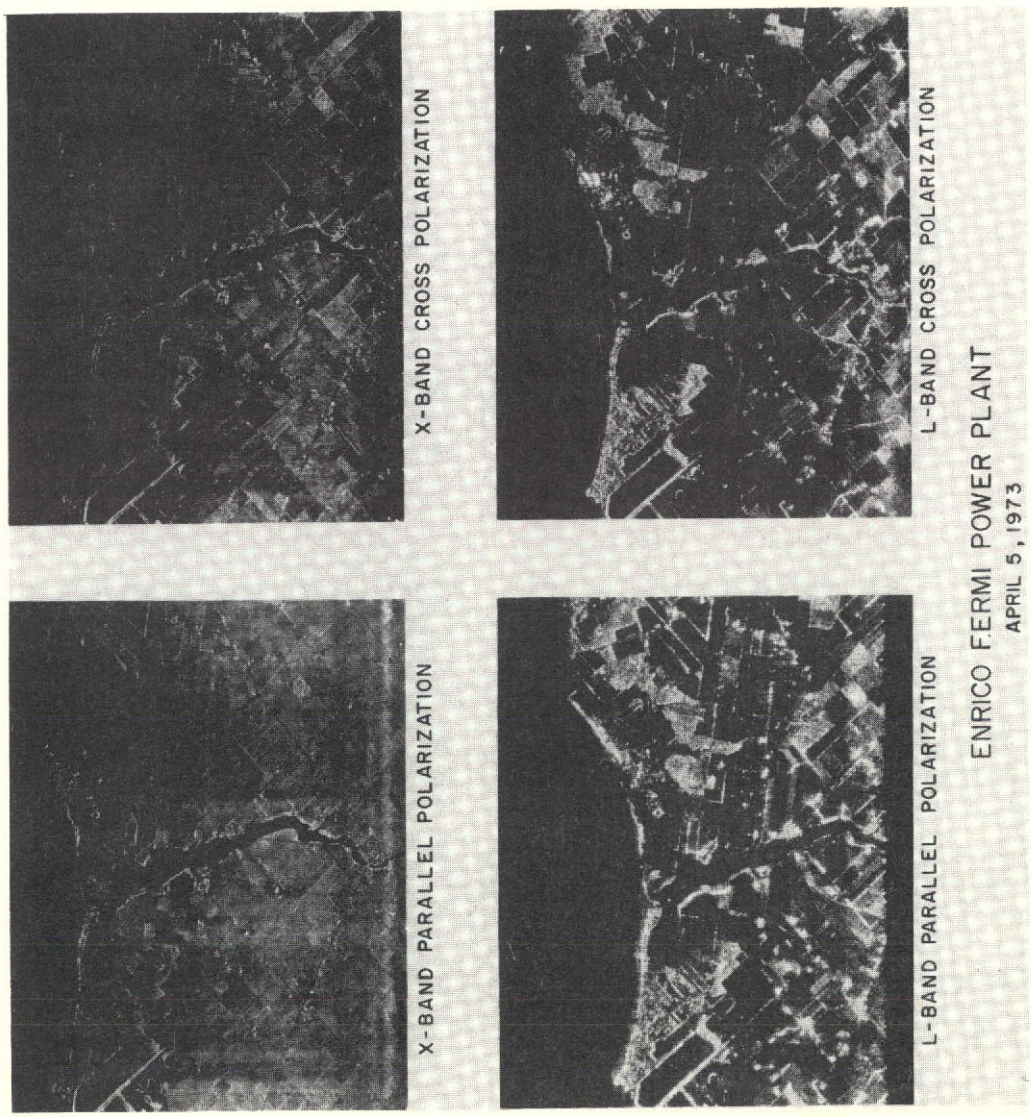

FIGURE 26. EXAMPLES OF DUAL-BAND RADAR IMAGERY

Many fields have considerable return at X-band and yet are imaged as dark or no-return areas at L-band. Image differences resulting from polarization are usually small enough to require detailed study of the imagery before they become apparent. In this imagery, however, some examples are fairly obvious to a casual observer in the fields southwest of the generating station.

10
SUMMARY AND CONCLUSIONS

A major reconfiguration of the airborne radar system was successfully completed under this contracted program. The magnitude of the modification and installation program was underestimated at the beginning. The development time required for several of the subsystems extended over longer periods than expected, and the installation of equipment in the aircraft was a more formidable problem than was predicted. Consequently, final installation of the complete system was not finished within the original timespan of the program plan; no time was left for test flights or equipment modification following these flights. Some of this system shakedown and debugging work was conducted under separate sponsorship; subsequent operation of the dual-band imaging radar during 1973 proved encouraging and useful multichannel radar imagery was generated.

REFERENCES

1. R. A. Rendleman, et al., Multifrequency Fine-Resolution Imaging Radar Instrumentation and Data Acquisition, Report No. 198200-1-F (NASA-CR), Environmental Research Institute of Michigan, Ann Arbor, Michigan, February 1974.
2. A. Kozma, E. N. Leith, and N. G. Massey, Tilted-Plane Optical Processor, Applied Optics, Vol. 11, No. 8, August 1972, p. 1766.
3. W. M. Brown, Synthetic Aperture Radar, IEEE Trans. Aerospace Elect. Sys., Vol. AES-3, March 1967, pp. 217-29.

DISTRIBUTION LIST

NASA Johnson Space Center
Space Sciences Procurement Branch
Houston, Texas 77058

ATTN: M. Krisberg/BB321 (1)
Contract NAS 9-12967

NASA Johnson Space Center
Technical Information Dissemination Branch
Houston, Texas 77058

ATTN: Retha Shirkey/BM6 (4)
Contract NAS 9-12967

NASA Johnson Space Center
Management Services Division
Houston, Texas 77058

ATTN: John T. Wheeler/BM7 (1)
Contract NAS 9-12967

NASA Johnson Space Center
Earth Observations Division
Houston, Texas 77058

ATTN: B. R. Baker/TF3
Contract NAS 9-12967 (4 + repro)